Master's thesis

NTNU
Norwegian University of Science and Technology

Brynjar Fagerli

Converter stress on transformer insulation materials

Master's thesis in Energy and Environmental Engineering
Supervisor: Kaveh Niayesh
Co-supervisor: Lars Lundgaard
December 2022

NTNU
Norwegian University of
Science and Technology

Brynjar Fagerli

Converter stress on transformer insulation materials

Master's thesis in Energy and Environmental Engineering
Supervisor: Kaveh Niayesh
Co-supervisor: Lars Lundgaard
December 2022

Norwegian University of Science and Technology

NTNU
Norwegian University of
Science and Technology

Preface

This master's thesis has been conducted at the Department of Electric Power Engineering at NTNU in Trondheim, in the fall of 2022. The project has been performed in close collaboration with SINTEF, through the project "FastTrans - Insulation stressed with fast rise time voltages from power electronics". The main objective of this study was to investigate how high-voltage insulation materials are affected by fast repetitive square voltage pulses compared to sinusoidal voltages. In addition, the insulation performance of the dielectric liquids Nytro 10XN and Midel 7131 was studied and compared.

I wish to thank my supervisor, professor Kaveh Niayesh at NTNU, and my co-supervisor Lars Lundgaard at SINTEF Energy Research, for their continuous support and guidance throughout the project work. Also, a huge thanks to Torstein Grav Aakre at SINTEF Energy Research for collaborating closely with me through the entire laboratory work and helping me learn how to use the measurement equipment.

I would also like to thank the people at the NTNU's mechanical and electrical workshops for providing self-customized equipment that was crucial for performing high-quality experimental tests in the laboratory.

Sammendrag

En økende andel teknologier som er koblet til strømnettet anvender kraftelektroniske omformere, både på forbruks- og produksjonssiden. Dette påvirker hvordan isolasjonsmaterialene til det elektriske utstyret i strømnettet belastes. Kraftomformere får stadig høyere vekslingsfrekvenser og kortere stigetider for å minimere effekttapene i energikonverteringer. Disse spenningene er i motsetning til tradisjonell 50 Hz sinusspenning, som det meste av elektrisk utstyr er dimensjonert for.

Denne studien sikter på å sammenligne hvordan disse to spenningsbelastningene fører til partielle utladninger (PD) i to ulike typer isolasjonsvæsker som benyttes i transformatorer. En grundig undersøkelse av karakteristikken til overflateutladninger (kalt streamere) i væske/presspan-isolerte systemer som blir utsatt for et svært divergent elektrisk felt ble utført. Isolasjonsmaterialet som ble brukt i laboratorietestene er basert på den mest vanlige typen transformatorisolasjon, nemlig dielektrisk væske i kombinasjon med væske-impregnert presspan. Med dette isolasjonssystemet, ble PD undersøkt ved å påføre spenning til en spisskantet elektrode.

Mineraloljen Nytro 10XN og den syntetiske esteren Midel 7131 ble brukt og sammenlignet i de eksperimentelle testene. For å teste isolasjonsmaterialene ble spenning i form av et gitt antall bipolare firkantpulser med varierende stigetider påført for hvert spenningsnivå, med spenningsverdier mellom 8 kV og 25 kV. I tillegg ble det utført tester med sinusspenning mellom 18 kV og 35 kV. For å innhente eksperimentelle data ble i hovedsak tre ulike målingsinstrumenter benyttet; fotomultiplikator (PMT), oscilloskop og intensivert CDD kamera. For å kvantifisere og sammenligne målinger som ble utført, ble PD-data fra oscilloskopet prosessert i MATLAB.

Utladningssannsynlighet og maksimal PD-amplitude ble funnet til å være høyere for kortere stigetider, for hvert gitte spenningsnivå i begge isolasjonssystemene. Videre var utladningssannsynligheten for positiv polaritet generelt høyere sammenlignet med negativ polaritet for begge isolasjonssystemene, bortsett fra sinusmålingene utført i Nytro, der utladningssannsynligheten for negativ polaritet var betydelig større. Maksimal PD-amplitude i Nytro var høyere sammenlignet med Midel for alle målinger basert på firkantspenning, men i sinusmålingene var det ingen tydelige forskjeller før 25 kV ble nådd. Fra og med 25 kV var maksimal PD-amplitude konsekvent høyere i Midel enn i Nytro for sinusmålingen. I Nytro ble en viskøs gelé dannet rundt elektrodespissen i løpet av hver måling, der mengden gelé korrelerte med størrelsen og mengden av utladninger. Denne geléen virket som et beskyttende skjold mot utladninger. Dette, sammen med romladningseffekten er antatt å være hovedårsaken til hvorfor sinusmålingene i Nytro skilte seg så mye fra de andre målingene. Resultatene indikerer også at høyere maksimale PD-amplituder i gjennomsnitt oppstår tidligere i forhold til påført firkantspenning i Nytro.

Til slutt ble en mer detaljert analyse av utladninger i Nytro (16 kV) og Midel (23 kV) utført. Resultatene viste at hver første utladning (bortsett fra én i Midel) på en ny lokasjon på elektroden i begge dielektrikum ble initiert i positiv halv-periode av påført spenning. Når en negativ utladning oppsto, var det i 58.8% (Midel) og 65.4% (Nytro) av tilfellene etter en positiv utladning hadde oppstått i foregående halvperiode av spenningen. Det var generelt færre halvperioder mellom hver utladning på en spesifikk lokasjon i Midel sammenlignet med Nytro. Dette bekrefter at Nytro er mer utsatt for romladningseffekt.

Abstract

An increasing amount of technologies connected to the power grid utilize power electronic converters, both on the consuming and generating side. This affects how the insulation materials of the electric equipment in the grid are stressed. The converters are approaching ever higher switching frequencies and shorter rise times to minimize the power losses in energy conversions. These stresses are contrary to the traditional 50 Hz sinusoidal voltages, which most electric equipments are dimensioned for. This study aims to compare how these two kinds of voltage stresses lead to partial discharges (PDs) in two different transformer insulation liquids. A thorough investigation of the characteristics of surface discharges (called streamers) in liquid/pressboard arrangements exposed to a highly divergent electric field was performed. The insulation material used in the laboratory tests is based on the most typical type of transformer insulation, namely dielectric liquid in combination with liquid-impregnated pressboard. With this insulation system, the PDs were investigated by applying voltage to a sharp-edged electrode.

The mineral oil Nytro 10XN and the synthetic ester Midel 7131 were used and compared in the experimental tests. To test the insulation materials, a predefined number of 30 Hz bipolar square voltage pulses with varying rise times was applied for each voltage level, with voltage values ranging from 8 kV to 25 kV. In addition, it was performed tests with 30 Hz sinusoidal voltages ranging from 18 kV to 35 kV. To obtain experimental data, three different measuring devices were utilized; photomultiplier tubes (PMTs), an oscilloscope, and an intensified CCD camera. To quantify and compare the measurements, the PDs were studied by post-processing data from the oscilloscope in MATLAB.

The discharge probability and maximum PD amplitude were higher for lower rise times, for every given voltage level in both dielectrics. Further, the positive polarity discharge probability was generally higher compared to the negative polarity discharges in both dielectrics, except for the sinusoidal measurements performed in Nytro, where the negative polarity discharge probability was significantly higher. The maximum PD amplitude in Nytro was higher than Midel for all the square voltage measurements, but in the sinusoidal measurement, there were no clear differences until 25 kV was reached. From 25 kV the maximum PD amplitude in Midel was consistently higher than in Nytro for the sinusoidal measurement. In Nytro, a viscous gel would form during every measurement, where the amount of gel correlated with the size and the number of discharges. The gel functioned as a protective shield against discharges. This, together with the space charge effect, was assumed to be the main reason why the sinusoidal measurements in Nytro deviated from the other measurements. The results also indicated that higher maximum PD amplitudes in Nytro occur earlier in relation to the applied square voltage.

Finally, a more in-depth analysis of discharges occurring in Nytro (16 kV) and Midel (23 kV) was performed. The results showed that every first discharge (except one in Midel) on a new location on the electrode in both dielectrics was initiated on the positive half-cycle of the voltage. When a negative polarity discharge appeared, it was in 58.8% (Midel) and 65.4% (Nytro) of the cases after a positive polarity discharge had occurred in the preceding half-period of the voltage. There were generally fewer half periods between each following discharge on a specific location in Midel compared to Nytro. This confirms that Nytro is more prone to the space charge effect.

Contents

List of Figures

List of Tables

1 Introduction

1.1 Background

One of the key factors in making the power grid smarter and more flexible is to incorporate more power electronic converters to control the power flow more effectively and to minimize power losses. There has been a big increase in grid-connected technologies utilizing power electronic converters, both on the consuming and generating side. Some examples of applications are electric vehicles, HVDC systems, FACTS devices, and UPS [1]. On the production side, renewable and non-dispatchable energy sources such as solar photovoltaic (PV) and wind power contribute to a substantial proportion of the power electronic converters in the power grid. Figure 1 and 2 shows the renewable energy production in the years 2000-2021 globally and in Norway, respectively.

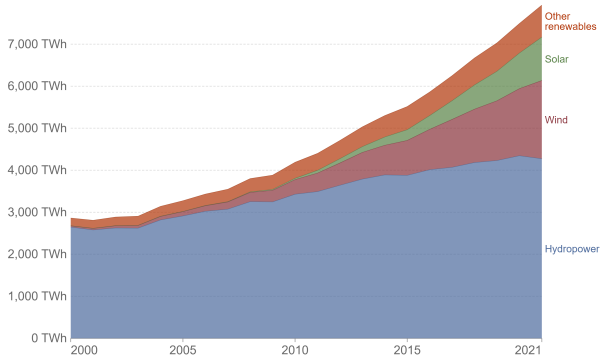

Figure 1: Global renewable energy production in the years 2000-2021 [TWh] [2].

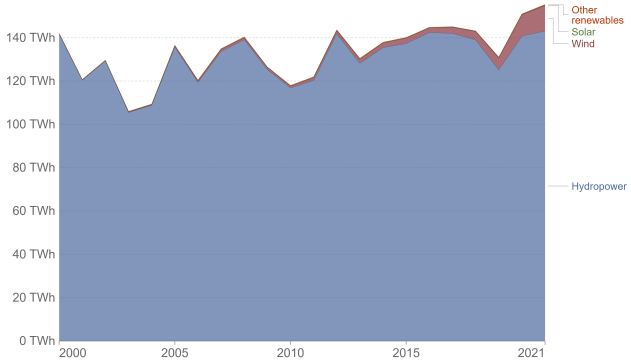

Figure 2: Renewable energy production in Norway in the years 2000-2021 [TWh] [2].

As can be seen, renewable energy production globally has more than doubled over the past 20 years, where PV and wind power represent an increasing proportion of the total power produced. Although Norway's energy production is heavily based on hydropower, there has been a big relative increase in installed wind energy capacity.

Considering the significant increase in grid-connected technologies using power electronic converters, the concern for how the high voltage insulation materials in the grid are stressed has become apparent. Research has indicated that voltages with faster rise times have a detrimental effect on the ageing mechanisms of the insulation system [3]. To quantify initial signs of degradation of high voltage insulation materials, PDs can be measured. During this master's thesis, the light signals emitted from the PD signals were measured optically using photomultiplier tubes.

1.2 Objectives of the master's thesis

This master's thesis aims to investigate the characteristics of surface discharges (called streamers) in liquid/pressboard arrangements exposed to a highly divergent electric field. The pressboards were impregnated by and immersed in two different kinds of dielectric liquids. The first is the mineral oil Nytro 10XN (hereafter Nytro), and the second is the biodegradable synthetic ester Midel 7131 (hereafter Midel). To test the insulation materials, a predefined number of 30 Hz bipolar square voltage pulses with

varying rise times were applied for each voltage level, with voltage values ranging from 8 kV to 25 kV. In addition, it was performed tests with sinusoidal voltages ranging from 18 kV to 35 kV. The positive and negative polarity discharge probability and maximum PD amplitude as a function of the voltage applied were obtained and studied. Further, pictures and oscillograms of discharges were looked into, as well as any visible ageing of the insulation materials. To quantify and compare these measurements, the discharges were studied by post-processing the data in MATLAB. The results were analyzed to provide a deeper understanding of the differences between Nytro and Midel impregnated insulation systems stressed by sinusoidal and square voltages. Also, plausible explanations for these differences were evaluated, such as the effect of gel formation, high field conductivity, and the space charge effect.

2 Literature Review

2.1 Power transformer insulation

Power transformers are critical devices in the power grid that facilitate the widespread transmission of electric energy in society. Optimal construction, operation, and maintenance of transformers are essential for providing a reliable supply of electric power to the end consumers. The design of the transformer insulation system is therefore vital, as a dielectric breakdown and a resulting short circuit may not only lead to a cut in energy supply but also involves considerable risk for components in the grid and the personnel operating them.

Dielectric oil in combination with oil-impregnated pressboards has been extensively used for over a century in power transformers. The two main objectives of the oil are to dissipate heat effectively and to electrically insulate the core to avoid short circuit currents [4]. Another beneficial dielectric property of the oil is its ability to prevent permanent cavity formations. This helps to stave off PDs, as the withstand capability of cavities is low compared to the rest of the insulation system [5]. The oil and pressboard barriers represent the main insulation between windings and ground and between adjacent windings [6].

Mineral oil is the most used insulating liquid in power transformers because of its excellent insulation properties and low cost [4]. However, due to its sub-optimal environmental traits, alternative dielectric liquids such as synthetic esters are aiming to replace mineral oil. One of the great advantages of using synthetic esters instead of mineral oil as the dielectric liquid is its ability to metabolise effectively in case of leakage to the environment. Midel can be classified as readily biodegradable, which means that it satisfies two criteria, as explained in [4]: The first is that after exceeding 10% degradation, 60% degradation must occur within 10 days. The second is that by day 28, 60% of the degradation must have occurred. Figure 3 clearly illustrates the superior ability of synthetic esters to degrade effectively compared to mineral oils. Another beneficial property of synthetic esters is their higher flash point and therefore lower inflammability compared to mineral oil. Synthetic esters can thus be considered a more safe dielectric liquid compared to mineral oil [4].

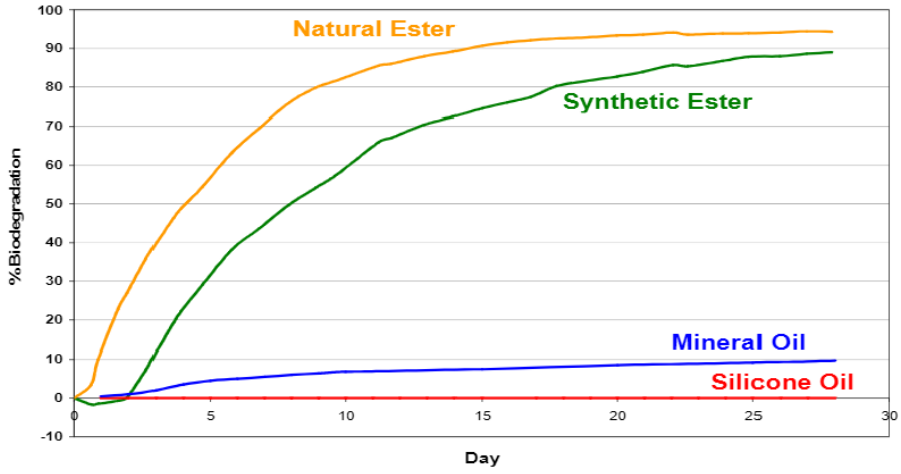

Figure 3: Biodegradability of dielectric liquids, retrieved from [4].

2.2 Partial discharge

PDs are transient, local dielectric breakdowns that occur in electrical insulation systems due to the electric field exceeding parts of the insulation's dielectric withstand capability [7]. The PDs can further deteriorate the insulation material and may ultimately lead to a complete dielectric breakdown [5]. For the test setup used in this study, there are mainly two types of PDs that are expected to occur, namely streamer discharges and void discharges. These PDs have some important characteristic differences. For void discharges, the initial free electrons are usually created due to the ionization of the gas inside the void. Streamers on the other hand, usually initiate and propagate from the electrode, at the region with the strongest inhomogeneous field.

In the experimental work for this thesis, it was not possible to perform measurements electrically in the square voltage setup, because of the large displacement currents created due to fast changes in voltage. The displacement current or capacitive current is proportional to the product of the capacitance of the test object and the change in voltage. The capacitance of the test object was measured to be 22 pF.

The frequency of this displacement current overlaps typical frequencies of PDs occurring on the test object, and it was therefore not possible to get accurate electrical measurements of the PDs which satisfy the IEC 60270 protocol. Therefore, the PD characteristics were measured optically, using a photomultiplier tube (PMT), which is explained in greater detail in section 2.2.2. A considerable effort was put into trying to calibrate the electrical measurements to the optical measurements, but unfortunately, this was not successful. Hence, the unit of measurement for the values obtained from the optical measurements is presented as *arbitrary unit* (a.u.). The theory behind measuring discharges electrically is left in the following section because it gives a better understanding of how PDs are formed.

2.2.1 Electrical measurement of PDs

To grasp how PDs can be measured electrically, an understanding of the physical mechanisms of PD formation in voids is helpful. For a PD to initiate in a void, the local withstand capability of the void needs to be exceeded to start a local electron avalanche. This requires free electrons in the void, which can be accomplished by ionization of atoms or by electron injection from the electrodes. Several mechanisms can facilitate the ionization of atoms, such as electromagnetic radiation, photo-ionization, and thermal ionization [7]. PDs result in energy losses which can be detected in the external circuit.

To understand how PDs are detected in the external circuit, the ABC-equivalent is a helpful model. Here, a void in the insulation can be modeled as a small capacitance C_c which is in series with a larger capacitance C_b which represents the insulation between the walls of the void and the upper and the lower electrode. The rest of the insulation is then modeled by C_c, which represents the largest capacitance. The ABC-equivalent circuit is illustrated in figure 4.

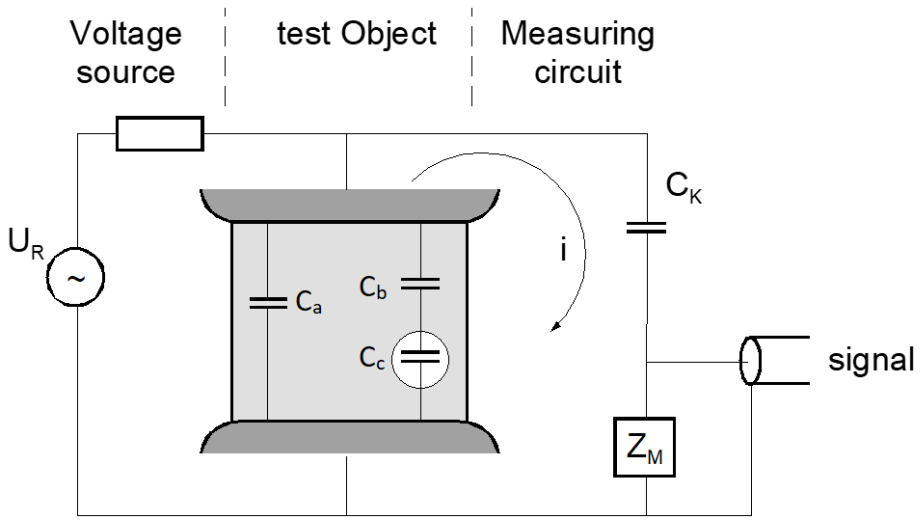

Figure 4: The ABC-equivalent circuit, reproduced from [7].

By voltage division, the voltage over the void (U_c) follows the applied voltage but is reduced with a factor $\frac{C_b}{C_b+C_c}$. If the applied voltage exceeds the withstand capability of the void, a local transient current will flow from one wall of the void to the other wall. [5]. The applied voltage at which PD initiates is referred to as the partial discharge inception voltage (PDIV). The corresponding voltage over the void is called the ignition voltage. As the discharge occurs, U_c instantaneously drops to approximately zero. To compensate for this sudden voltage drop, the external circuit supplies a transient current to the test object, which is represented by i in figure 4. This charge injection is usually fed primarily by a relatively big coupling capacitor (C_K) in parallel with the test object. The charge carried by i is normally denoted by apparent charge and can be detected by connecting a suitable measuring impedance (Z_M) in series with the coupling capacitor. It is called apparent charge because the measured charge does not represent the actual discharge current inside the void, but is proportional to it and can be calculated by proper calibration. [5, 7]

2.2.2 Optical measurement of PDs

PMTs are photosensitive apparatuses that are able to convert electromagnetic signals into electrical signals that are further amplified. This ultimately enables quantification of the radiant energy that was emitted from the object of interest. The signal frequencies in the electromagnetic spectrum that can be detected, usually correspond to ultraviolet, visible, and infrared radiation [8]. A PMT was used together with an oscilloscope to spot and quantify the light emission occurring during a PD inside the transparent insulating liquid on the surface of the pressboard. Figure 5 shows schematically how the PMT works.

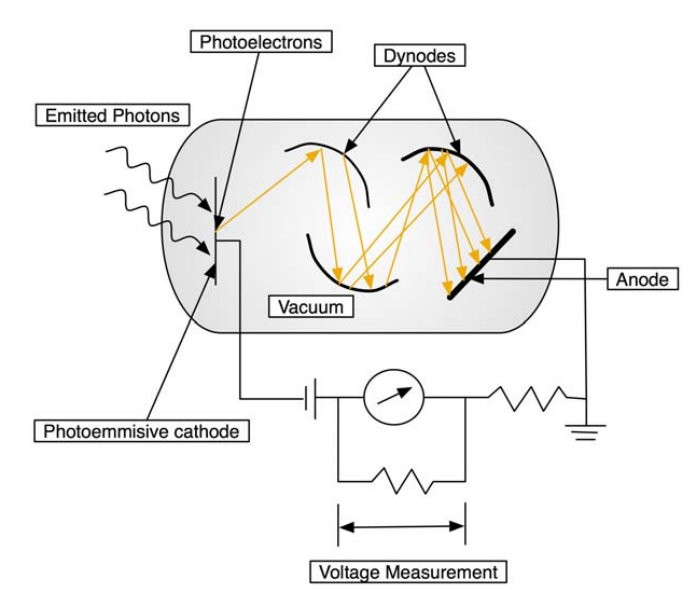

Figure 5: Schematic illustration of the PMTs functionality. Retrieved from [9].

Photons emitted from the streamers will hit the photoemissive cathode, which in turn releases photoelectrons by means of the photoelectric effect. Then these electrons reach the dynodes, which amplify the number of electrons due to the applied voltage. Further, this leads to a cascading effect, where the number of electrons is multiplied for each dynode encounter. After the final dynode, the electrons reach the anode, where a current is produced and ultimately provides a voltage measurement that is proportional to the light intensity emitted from the discharge. [9]

2.3 Streamers in dielectric liquids

Streamers are a specific type of PD that originally was a synonymous term with gas discharges. Later it has also come to include discharges occurring in highly inhomogeneous electric fields in dielectric liquids [5]. A crucial distinction between void discharges and streamers is the PD initiation mechanism. For void discharges, the initial free electrons are usually provided inside the void by ionization of the gas inside. Streamers, on the other hand, will always initiate due to electron emission from the electrode and propagate through the liquid from there. When streamers first initiate in a dielectric liquid, a transient current pulse is produced due to the formation of a conductive, ionized gas phase. This current pulse leads to heat losses, which then evaporates the liquid and expands to form a conductive tree-like gas channel. [4]

The initiation and propagation of streamers in liquids depend on different parameters. For instance, the propagation speed is highly dependent on the applied voltage, field configuration, and chemical composition, and may range from 100 m/s up to 100 km/s. Initiation is more dependent on the maximum electric field, liquid type, moisture content, presence of space charges, bubbles, or solid particles in the liquid. Having a solid barrier such as a pressboard impacts both initiation and propagation. The pressboard works most effectively as a barrier against streamer formation when it is placed close to the sharp electrode. [4]

2.3.1 Positive vs negative polarity streamers

It is important to distinguish between positive and negative polarity streamers, as they have different characteristics due to the difference in direction of the applied electric field. The differences in streamer characteristics are largely due to the formation of space charges around the sharp electrode, effectively extending or abbreviating the size of the anode or cathode. Both the streamer inception voltage and the streamer structures have been found to be affected by the developing space charges [10].

In strongly inhomogeneous electric fields, negative polarity streamers normally have lower PDIV compared to positive polarity PDIV. Positive polarity streamers normally have higher PD amplitudes and higher streamer stopping lengths compared to negative polarity streamers, for the same applied voltage [5]. A sharper electrode also creates a stronger inhomogeneous field around the tip of the electrode, which together with a longer voltage duration facilitates space charge formation there [4]. The characteristic differences between positive and negative polarity streamers are clearly shown in two recent studies about oil/pressboard discharges under divergent AC voltage [11, 12]. Here, at a constant voltage, the PD repetition rate was clearly higher for negative polarity streamers, while the PD amplitudes were considerably higher for positive polarity streamers.

When a voltage of alternating polarity is applied to an insulating liquid, positive and negative polarity space charges are expected to develop around the edge of the sharp electrode [10]. Since the drift velocity of positive ions is generally slower than for electrons, a net positive charge accumulation may occur around the sharp edge. Thus, the space charge effect shown in figure 6 is considered representative of the setup used in the measurements, and the field strength distribution from the anode to the cathode may also be regarded as realistic [5]. As seen in the figure, when the sharp electrode is positive, there will also be positive charge accumulation around the tip of the electrode. This results in a field reduction around the tip, and is referred to as the Poisson field. The graph illustrated without space charges is referred to as the Laplacian field.

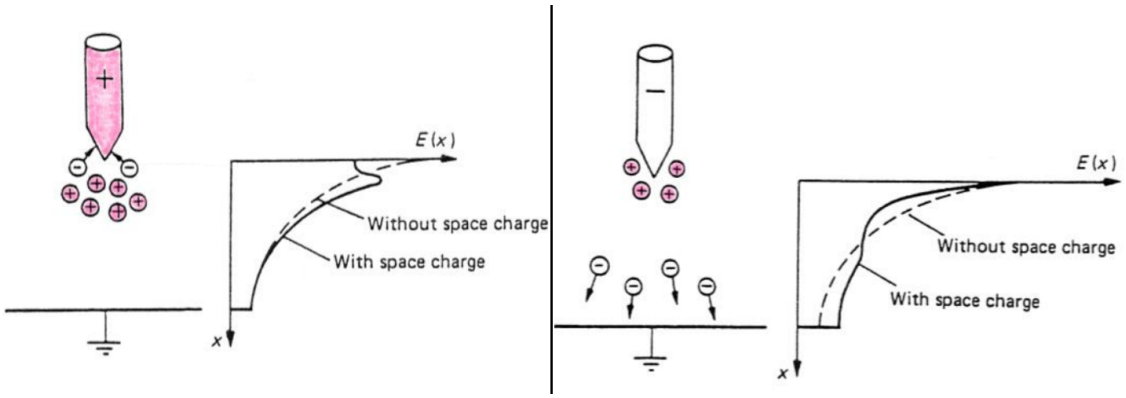

Figure 6: The effect of space charges in a needle to plane arrangement, with the resulting electric field distribution [5]. Left: Positive needle. Right: Negative needle.

2.4 Mineral oil vs synthetic ester

A master's thesis written by Skirbekk was performed by using a very similar test object as the one used in this master's thesis [13]. As seen in figure 7, she found that the optically measured PDIV was slightly larger for Midel compared to Nytro, for both sinusoidal and bipolar square voltage measurements. However, the procedure for obtaining the PDIV for the voltage measurements differs from the method used in this master's thesis. Skirbekk had a typical PDIV definition, in which the PDIV represents the voltage level at which the first PD was observed for the whole measurement. In this master's thesis, however, this was obtained by making discharge probability curves instead. The procedure for obtaining this is thoroughly explained in section 3.4.3.

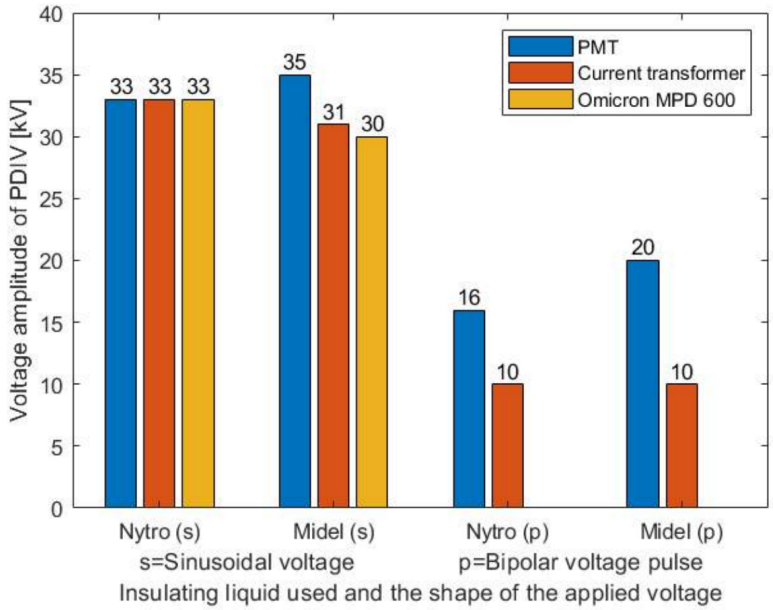

Figure 7: Measured PDIV for Nytro and Midel. Retrieved from [13].

In the project preceding this master's thesis, the PD repetition rate and the maximum PD amplitude in Nytro 10XN and Midel 7131 were measured electrically, as seen in figure 8 and 9 [14]. As can be seen, the PD repetition rate is higher in Nytro for the first 5 voltage levels, then Midel exceeds Nytro and keeps increasing at a much faster speed. The maximum PD amplitude is generally higher in Midel and the difference increases for every voltage level. Further, the positive polarity PD repetition rate and maximum PD amplitude were generally higher compared to the negative polarity discharges in both dielectrics, except for the PD repetition rate in the sinusoidal measurements performed in Nytro, where the negative polarity PD repetition rate was consistently much higher compared to the positive polarity.

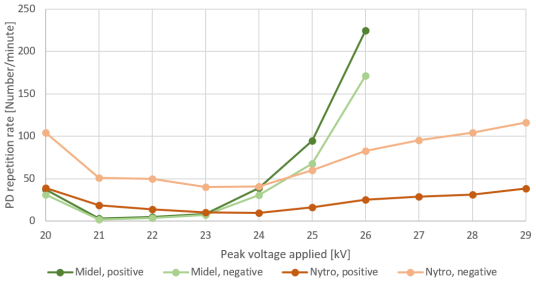

Figure 8: PD repetition rate [Number/minute] as a function of applied voltage in Midel and Nytro [14].

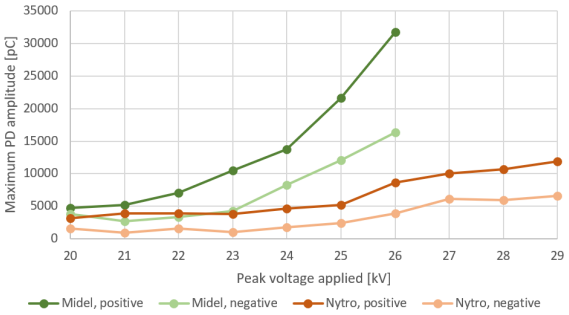

Figure 9: Maximum PD amplitude [pC] as a function of applied voltage in Midel and Nytro [14].

Although the exact same test object was used in the project preceding this thesis, there were two crucial differences in that study. The first is the voltage source, which in the previous project was solely based on a purely sinusoidal, 30 Hz voltage source in contrast to bipolar square voltage pulses. The second difference is the measurement technique, which in the preceding project was done electrically and not optically, as in this master's thesis.

As shown in table 1, Nytro 10XN and Midel 7131 have some different quantifiable properties [15]. The conductivity and viscosity are the main differences between the two dielectric liquids. These parameters have partly been used to explain the differences in results obtained in this thesis, as presented in section 4.

Parameter	**Unit**	**Nytro 10XN**	**Midel 7131**
Relative permittivity	[1]	2.17	3.17
Conductivity	[pS/m]	0.60	23.61
Density	[kg/m^3]	872	970
Viscosity	[mm^2/s]	7.6@40°C	28@40°C

Table 1: Values for relative permittivity, conductivity, density and viscosity in Nytro 10XN and Midel 7131 [15].

Additional studies comparing Midel and Nytro stressed by square voltage pulses could not be found, hence, the rest of this section contains a more general literature review on mineral oil compared to synthetic esters stressed by AC voltages.

The PhD study by Wang gave great insight into how well the synthetic ester *Midel 7131* performs as an insulating liquid compared to the mineral oil *Gemini X*. A big part of the thesis is focused on investigating the PDIV of both dielectric liquid types, without the use of a pressboard perpendicular to the electric field. By utilizing a point-to-sphere electrode arrangement and increasing the 50 Hz AC applied voltage by $1kV_{peak}$ per step, both the PD repetition rate and maximum PD amplitude were recorded, as seen in figure 10 and 11. The distance between the electrodes was 50 mm and the spherical electrode had a diameter of 12.5 mm. For both Midel and Gemini X, the maximum PD amplitude is quite similar for every voltage level and seems to have a linear increase. [10]

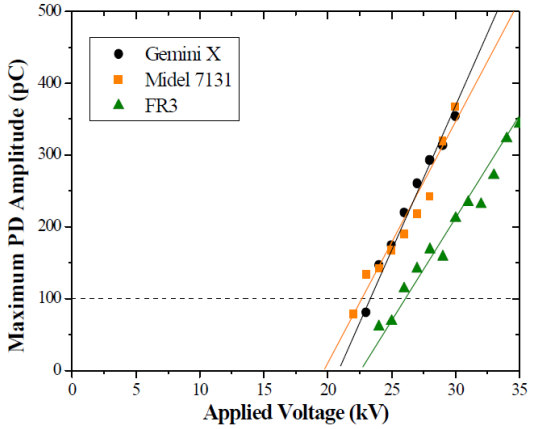

Figure 10: Maximum PD amplitude [pC] for three different dielectric liquids [10].

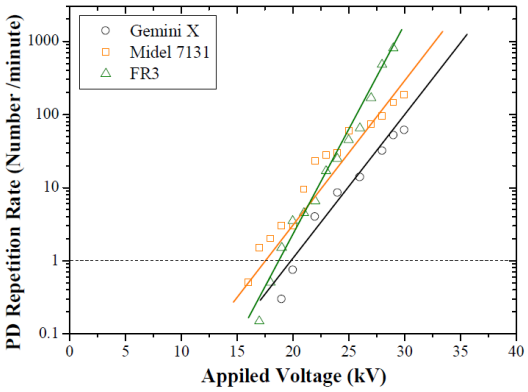

Figure 11: PD repetition rate [Number/minute] for three different dielectric liquids [10].

The PD repetition rate, on the other hand, is clearly higher for Midel compared to Gemini X. As the y-axis is logarithmic and the x-axis is linear, the PD repetition rate can be approximated to have exponential growth for both the mineral oil and the synthetic ester. These curves were used to approximate the PDIV of the liquids, where a differentiation was made between *industrial PDIV* and *academic PDIV*. The former was based on figure 10 while the latter was based on figure 11. Both the industrial and the academic PDIV found a slightly higher PDIV for the mineral oil compared to Midel. [10]

Previous work performed by Beroual also indicated that the average number of PDs N and maximum PD amplitude were considerably higher for pressboard/vegetable oil compared to pressboard/mineral oil when a certain voltage threshold was exceeded. With a pressboard thickness of 2 mm and a voltage application of 16.5 kV AC at 50 Hz, it was clearly shown that both N and the maximum PD amplitude were much higher for vegetable oil compared to mineral oil. The same study also showed that the maximum PD amplitude increases when the pressboard thickness decreases. The study also found that the maximum PD amplitude would be approximately equal for both pressboards based on vegetable oil and mineral oil up to a certain voltage level. For instance, for a pressboard thickness of 4 mm, there was observed no difference in the maximum PD amplitude up to 25 kV. [16]

The CIGRE report in [4] on the other hand, concluded that PDIV for mineral oil and synthetic esters are of similar magnitude. All of these partly coinciding and partly contradicting findings confirm the need for additional research on the PD characteristics of mineral oils compared to synthetic esters.

2.5 Parameters affecting PD formation

When performing PD measurements on insulating materials, it is paramount to have a thorough understanding of all the parameters that affect the accuracy of the results that are obtained. There will always be limitations to the ability to mitigate sources of error in the measurements. However, reducing the impact of these will make it easier to interpret the results, as several of the parameters can to a varying degree be neglected. In the following, the most important parameters affecting PD formation

are presented. This is further used as a justification for the measuring procedures used in the laboratory experiments, as presented in chapter 3.

The rate of ageing of oil-impregnated paper is roughly proportional to its moisture content [5]. This is due to the increase in dielectric losses and the resulting temperature rise that occurs when the moisture content increases. The moisture content also degrades the cellulose by shortening the chain molecules and as a consequence becomes more fragile [17]. The breakdown voltage as a function of relative moisture content for dielectric liquids such as mineral oil and synthetic ester is presented in figure 12 [18].

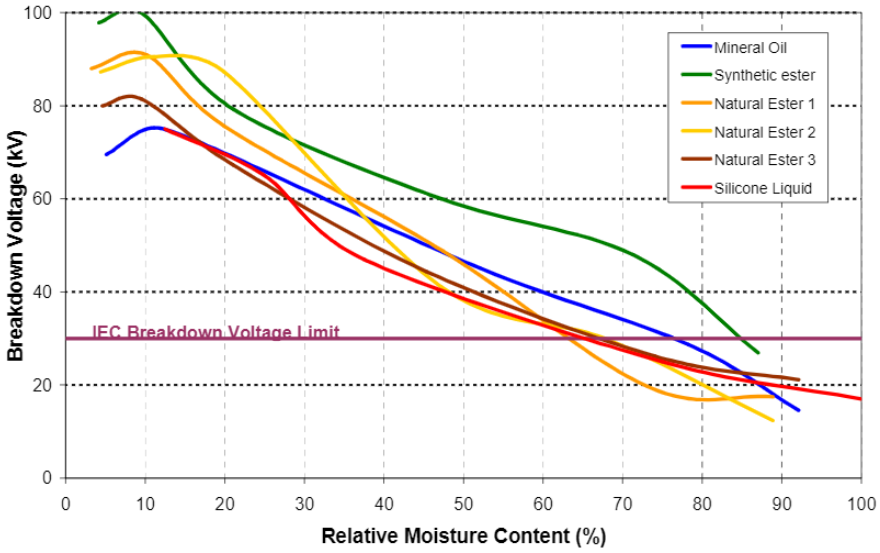

Figure 12: Breakdown voltage as a function of relative moisture content of different dielectric liquids [18].

As already suggested in section 2.3, a small degree of particle contamination has little to no effect on the propagation of streamers in mineral oil stressed by AC divergent fields [4, 10]. Some studies have actually shown that the presence of movable carbon particles stressed by an AC divergent field, increases the dielectric withstand ability of mineral oil due to space charging of the carbon atoms [19]. However, the initiation of the streamers (PDIV) is highly affected by particle contamination. Especially metallic particles will reduce both the PDIV and the breakdown strength of the insulation system considerably [5].

Further, gas bubbles can cause more PDs to initiate, due to the relatively low dielectric strength of the gas. When the withstand ability of the gas is exceeded, gas discharges will occur. The electrode curvature also affects the initiation of PDs greatly, as a sharper electrode will create a stronger inhomogeneous electric field which reduces the PDIV of the insulation system. However, the breakdown strength is not affected much by the electrode curvature, as that is more dependent on the total voltage over the test object. [5]

2.6 Square voltage characteristics

Repetitive square voltage pulses from power electronics have certain properties that can be characterized by their duty cycle, rise time, switching frequency, and polarity. The duty cycle is the ratio between the time of the active signal versus the total time of one period. The polarity of each pulse can be either positive or negative, depending on the desired output signal. The rise time is defined as the time it takes for the voltage pulse to go from 10% to 90% of its peak value. This is illustrated in figure 13, where the rise time is denoted as t_r. This figure also shows the overshoot and undershoot phenomenon, which represents the maximum swing above and below the desired value. This phenomenon was to a varying degree present during the laboratory measurements, and its specific value depended on both the voltage level and the rise time. [20]

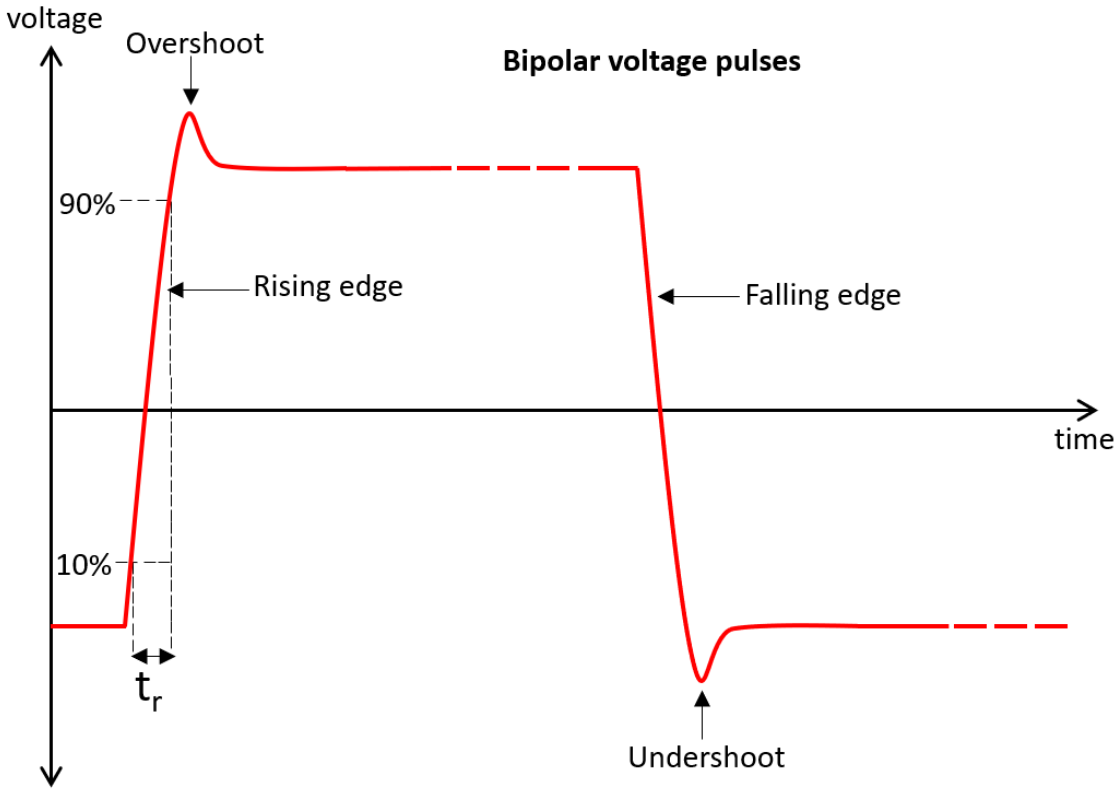

Figure 13: Figure showing the shape of bipolar voltage pulses. The overshoot and undershoot, along with the rise time are illustrated.

Several scientific papers have indicated that shorter rise times lead to lower PDIVs and higher maximum PD amplitudes. As seen in figure 14, the maximum PD amplitude of a point-plane geometry stressed with square voltages with fast rise times are significantly higher compared to the square voltages with slow rise times [21]. The same tendency was confirmed in [22], which studied a greater amount of rise times. Figure 15 shows that lower PDIVs are observed for faster rise times, and the PDIV also seems to be inversely proportional to the switching frequency.

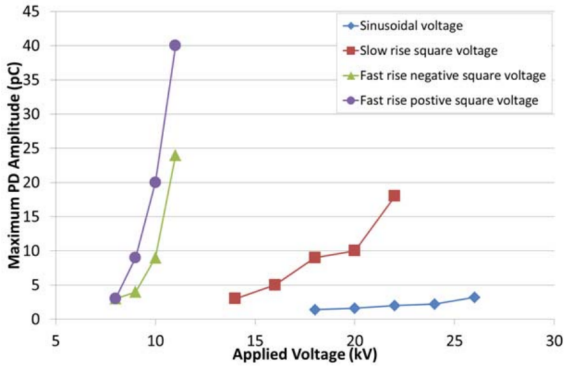

Figure 14: Maximum PD amplitude for square and sinusoidal voltages in a point-plane geometry. Fast rise time=100 ns. Slow rise time=400μs. [21]

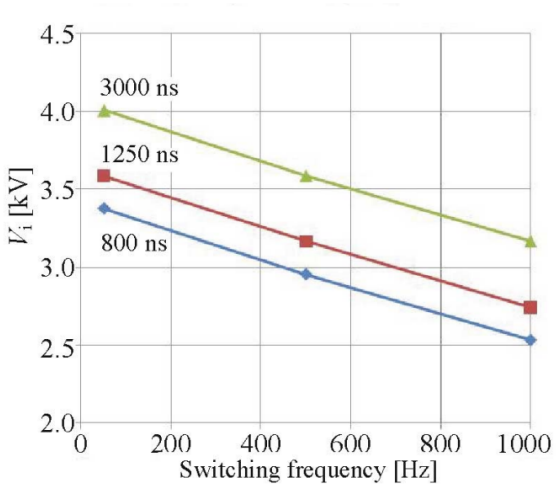

Figure 15: PDIV as a function of switching frequency and rise times [23].

As seen in figure 16, the majority of the PDs occur around the rising and falling edge of the bipolar voltage pulses. This tendency was discovered in most of the measurements in the current study as well, and this was used to appropriately set the settings on the oscilloscope, as presented in section 3.4.3.

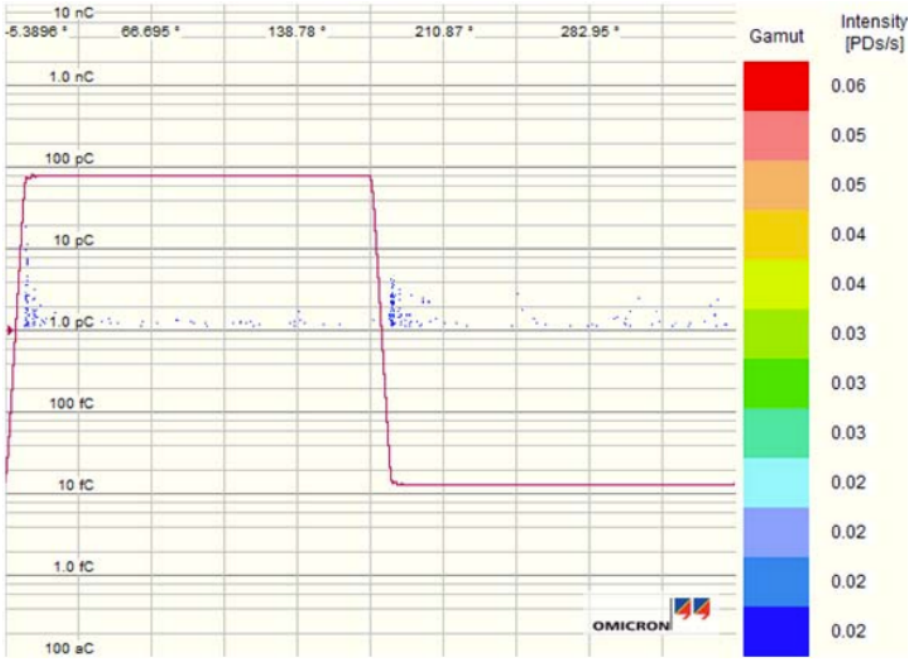

Figure 16: Optical PD pattern for slow rise time square voltage at 18 kV.

3 Method

The following sections provide detailed information about the test setup for the square and the sinusoidal voltage system, sample preparation, test object, and the test procedure. The method used in the laboratory is quite similar to what Skirbekk did in her master's thesis in spring 2020 [13]. However, some necessary changes were made for this study, as Skirbekk encountered some problems. For instance, one of the problems was having the breakdown voltage too close to the PDIV [13]. In this study, this was avoided by increasing the diameter of the pressboard, such that the streamer had to propagate over a longer distance to achieve a dielectric breakdown.

In both the square and the sinusoidal voltage test setup, the test object was confined in a metal cabinet. This cabinet could be regarded as an approximate Faraday cage since the metal cage functions as a closed conducting shell. As [24] states: "If the field outside the cage is changed, the charge on the cage walls will redistribute itself so that the field inside will remain zero". Thus, the electrical noise and light pollution originating from outside of the cabinet was minimized.

3.1 Test setup

3.1.1 Square voltage system

A picture of the physical laboratory test setup is shown in figure 17, with all the relevant measuring devices that play a role in the collection of data in the experiments. Figure 18 schematically shows the test circuit logic for obtaining PD measurements optically. To visually inspect the streamer propagation characteristics, pictures were taken when the discharges occurred in the measurements. To achieve this, the Lambert HiCAM 500 camera was installed over the test object and pointed down at it. After adjusting the focus on the camera so that the surface of the pressboard was clear, the Lambert Intensifier Control Software and TimeViewer could be utilized to adjust the frame rate and exposure time to take optimal pictures of discharges with the camera. The gain level on the camera was set to 750 on the measurements performed with Nytro and 600 in Midel.

To produce square voltage pulses to stress the test object, capacitor banks (C_B=5 nF) of opposite polarities were charged by two distinct DC voltage sources at a set frequency of 30 Hz. The resistor R_{lim} was set both to limit the current and to achieve the desired rise time of the output voltage, where lower values gave faster rise times. For the measurements performed in this study, R_{lim} was set to either 200 Ω or 1500 Ω. This gave rise times of about 50 ns and 300 ns, respectively. The resistances R_C had a value of 450 kΩ. As indicated in figure 17 and 18, the camera, the PMT, and the test object (T.O.) were placed inside the metal cabinet.

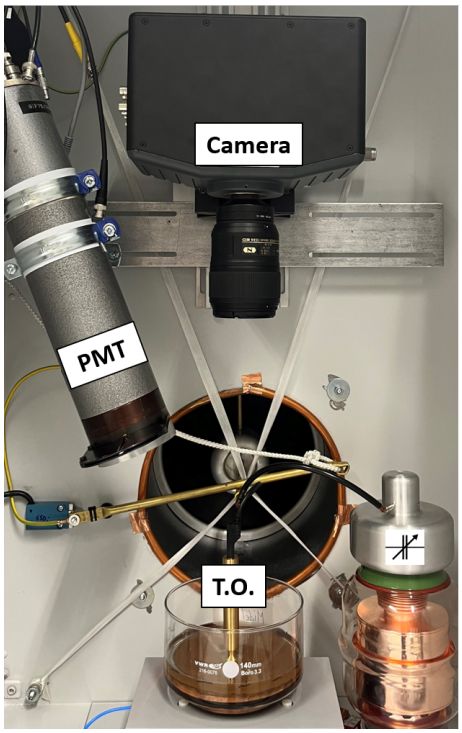

Figure 17: Illustration of the square voltage test setup inside the cabinet.

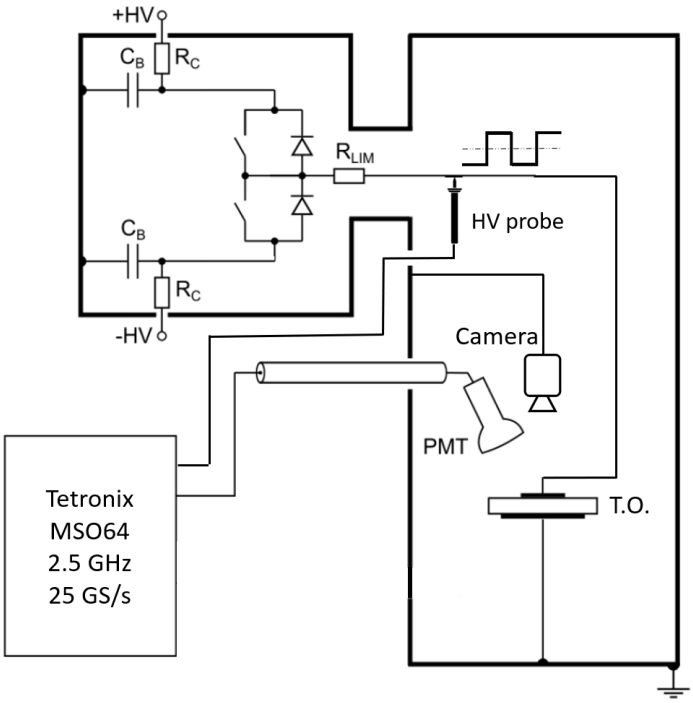

Figure 18: A schematic view of the test equipment and measurement devices in the square voltage test setup. This is a modified version from [25].

3.1.2 Sinusoidal voltage system

A picture of the laboratory test setup is shown in figure 19, with all the measuring devices used in the experiments. Figure 20 schematically shows the test circuit logic for obtaining PD measurements optically. The measurement parameters were adjusted using the Tektronix AFG3052C signal generator by manually turning a dial to achieve the desired output voltage. The frequency was set to 30 Hz and the output impedance was set to *high*. 30 Hz was the resonance frequency of the test set-up [13]. At this frequency, the load impedance is considered purely resistive and thus ensures low reactive power consumption and little harmonic distortion [26].

As figure 19 and 20 shows, the PMT, the T.O., the HV transformer, and the coupling capacitor are placed inside the metal cabinet. The PMT was placed directly above the test object and pointing down towards it to receive any photons that are emitted from the test object due to discharges.

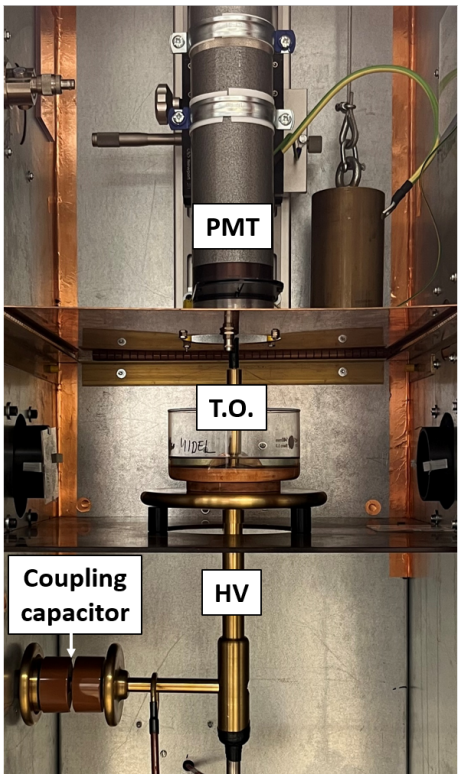

Figure 19: Illustration of the sinusoidal voltage test setup inside the cabinet.

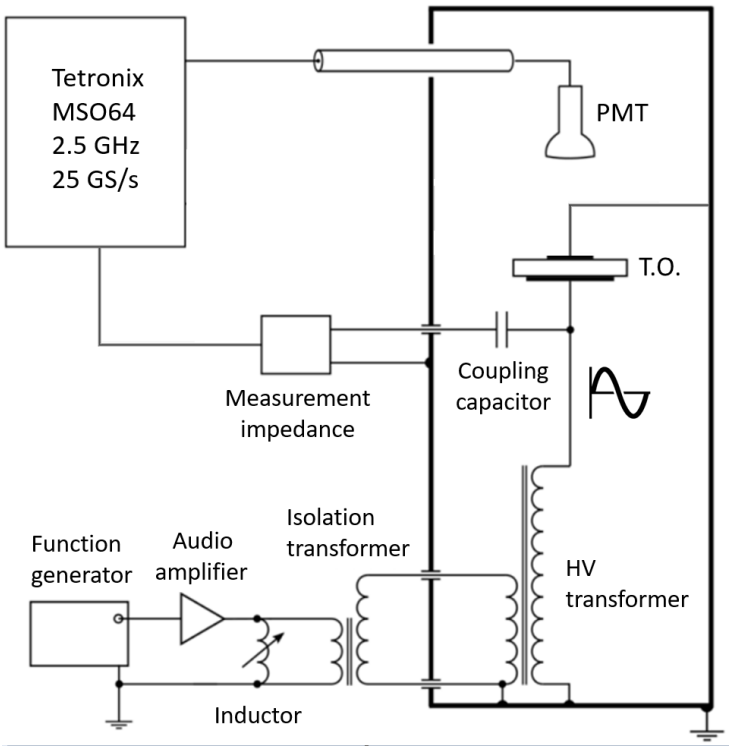

Figure 20: A schematic view of the test equipment and measurement devices in the sinusoidal voltage test setup. This is a modified version from [25].

3.1.3 The oscilloscope

As shown in figure 21, the Tektronix MSO64 mixed signal oscilloscope was used to obtain all the relevant discharge data for optical measurements. By making the oscilloscope trigger on the rising and falling edge of the applied voltage, the oscilloscope would display all the optical discharges for all the voltage half-periods in a set amount of time. Triggering on the rising and falling edge was beneficial, as this made it possible to inspect any correlation between PDs in two consecutive voltage half-periods.

The oscilloscope setting called *Fast frame* was used to trigger a set amount of times, as explained in [27]. The time window for each trigger was set based on a trade-off between the resulting file size, the required time resolution for PD analysis, and when PDs typically occurred in relation to the applied voltage. A thorough justification for the settings on the oscilloscope is given in section 3.4.3. The discharge waveform for each discharge picture was obtained by synchronizing the oscilloscope with the high-speed camera, referred to as *Camera triggering* in figure 21.

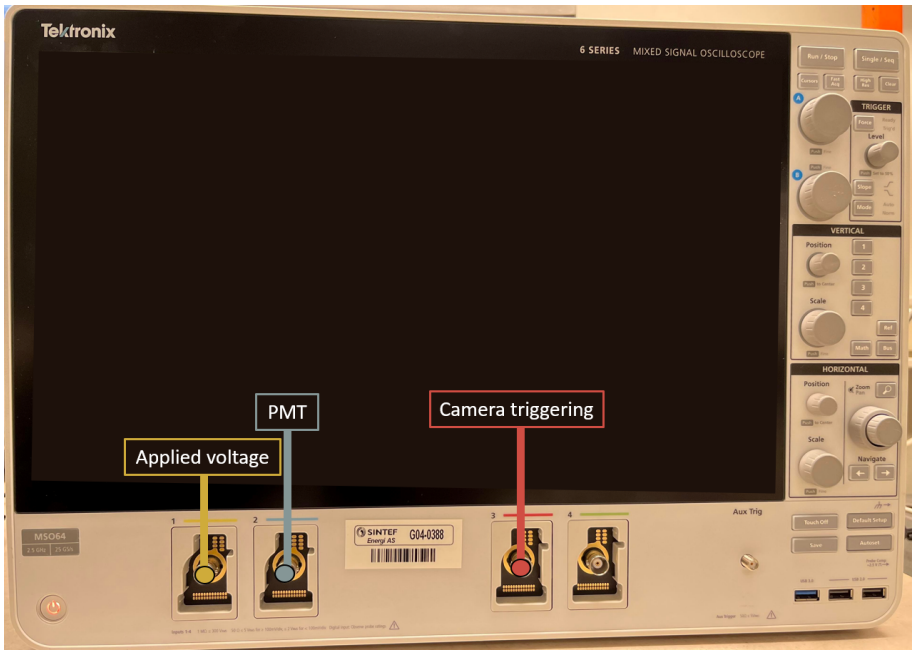

Figure 21: The Tektronix MSO64 mixed signal oscilloscope used in the measurements. The connections to the channels used are specified.

3.2 Sample preparation

The sample preparations were carried out using mainly the same technique as the project preceding this thesis [14]. The procedure from the project report is partly presented in this section. Before the pressboards could be tested, they needed to be properly prepared. Firstly, the pressboards had to be dried to ensure a sufficiently low moisture content in the pressboards. This is crucial, as the rate of ageing is approximately proportional to the moisture content [5]. The drying process was performed by placing the pressboards and the dielectric liquids in a vacuum heating cabinet. The pressboards were dried under vacuum for about 3 days at 120 °C. Nytro and Midel were dried under vacuum for 4 days at 70 °C and 60 °C, respectively. Further, the pressboards needed to get vacuum impregnated with the dielectric liquid, as shown in figure 22. As can be seen, a tube is connected from the glass lid to a vacuum pump. The vacuum pump ensured that no unwanted air bubbles or moisture entered the insulation system during impregnation.

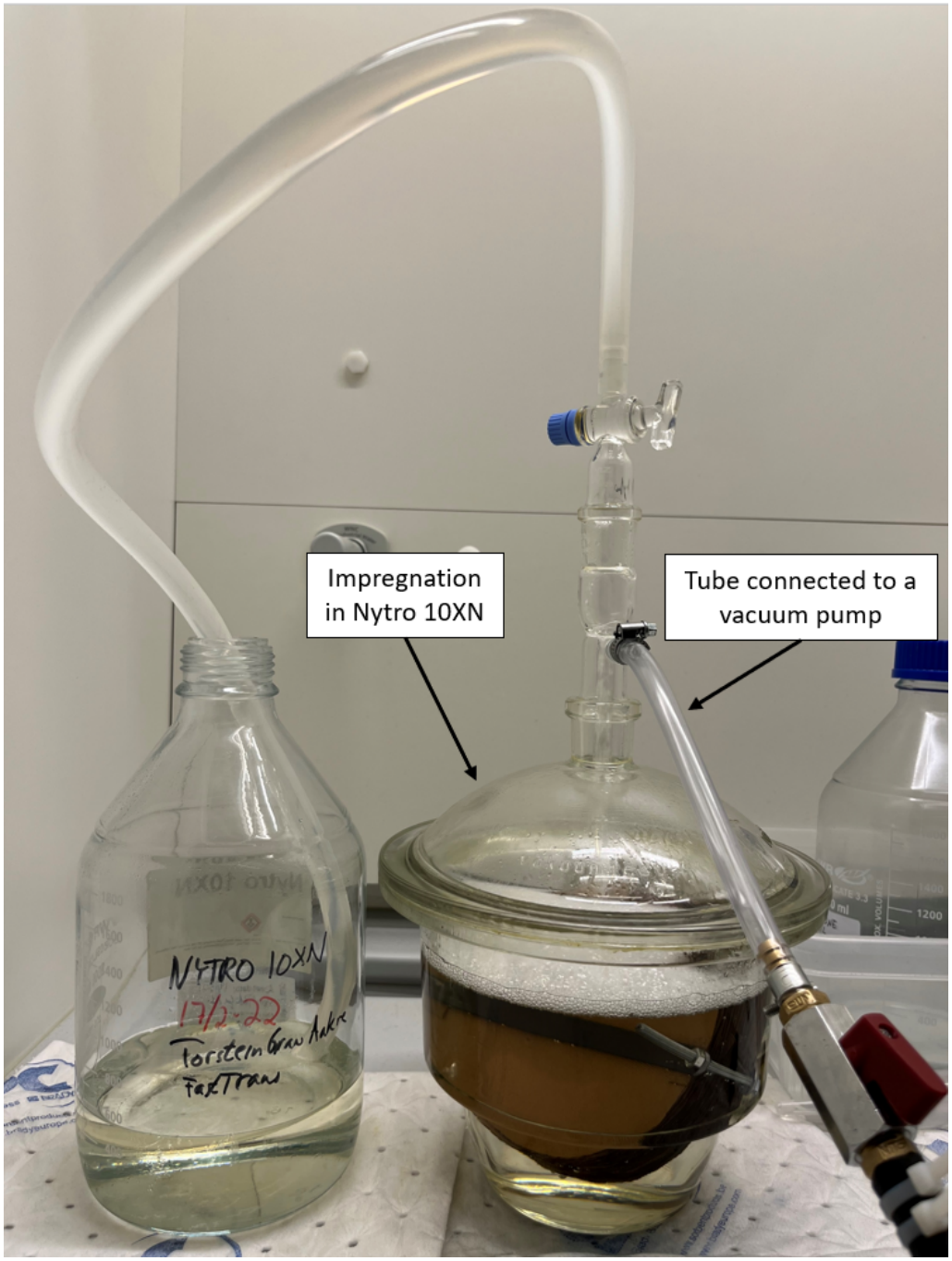

Figure 22: Vacuum impregnation of pressboards, immersed in Nytro 10XN.

As seen, the pressboards got completely immersed in the dielectric liquid inside the desiccator. This made sure that the pores of the pressboard were saturated with the liquid, hence preventing internal PD initiation in cavities when testing [5]. The last step before a measurement could be carried out, was to add fresh dielectric liquid and the liquid-impregnated pressboard into a glass dish. The glass dish was then put under vacuum for 2-4 minutes since air would easily enter the dish and get trapped underneath the pressboard. The glass dish is shown in picture number 3 in figure 23.

3.3 Test object

Figure 23 shows details about the test object used in the laboratory, namely the electrode, pressboard, dielectric liquid, and glass dish. As shown in figure 23 in picture number 3, the pressboard is placed directly under and perpendicular to the electrodes and the resulting electric field.

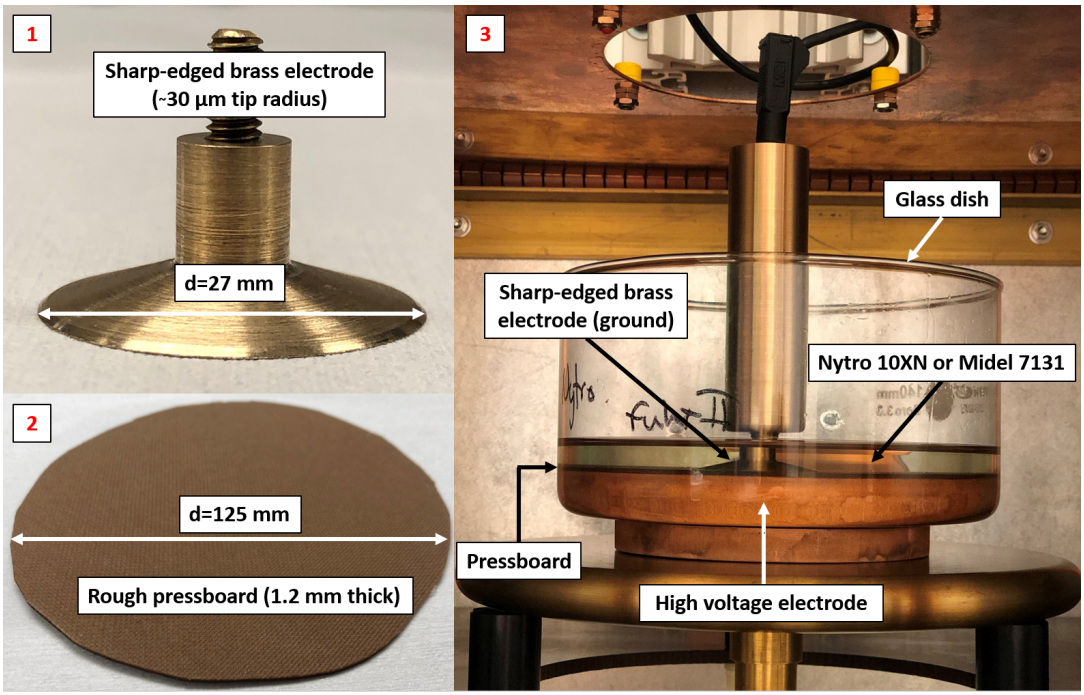

Figure 23: **1:** The sharp-edged brass electrode **2:** The rough pressboard **3:** The test object placed inside the test cabinet. The brass electrode is submerged in dielectric liquid and is placed on top of a pressboard.

The diameter of the pressboard was set to 125 mm. The electrode used in the laboratory was a sharp-edged brass electrode, providing a strong inhomogeneous electric field. The diameter of the bottom of the electrode is 27 mm. As the field strength around the edge of the electrode is highly dependent on its sharpness, the curvature radius of the electrode edge was measured using a microscope, achieving a reasonably precise measure of its curvature. The curvature was found to be approximately 30 μm. Using a capacitance meter, the capacitance of the test object was measured to be 22 pF.

3.3.1 Moisture content of the pressboard

Cellulose is a highly hygroscopic material, hence, the main part of the moisture will be in the pressboard part of the insulation. Therefore the moisture content of the liquid was neglected and only the moisture content of the pressboard was measured [5]. Karl Fischer titration was used to measure the moisture content of the pressboard. It is worth noting that the most important aspect was not minimizing the moisture content, but knowing the value. The moisture content of both the Midel and Nytro-impregnated pressboards used in the measurements were found to be 0.4 %. Since the moisture content is below 0.5 %, it is dry insulation, as defined in [28].

3.4 Test procedure

3.4.1 Noise signals

Measurements of PDs will inevitably contain a certain degree of undesired noise signals. As figure 24 illustrates, there are numerous sources of noise that can be especially difficult to avoid when measuring PDs in the power grid [7]. Having the test object confined in a metal cabinet under relatively controlled circumstances in a laboratory made it easier to restrict the harmful effect the noise would have on the accuracy of the measurements. The measurements performed by the PMT are especially sensitive to light, so a big emphasis was put on keeping it sufficiently dark inside the cabinet.

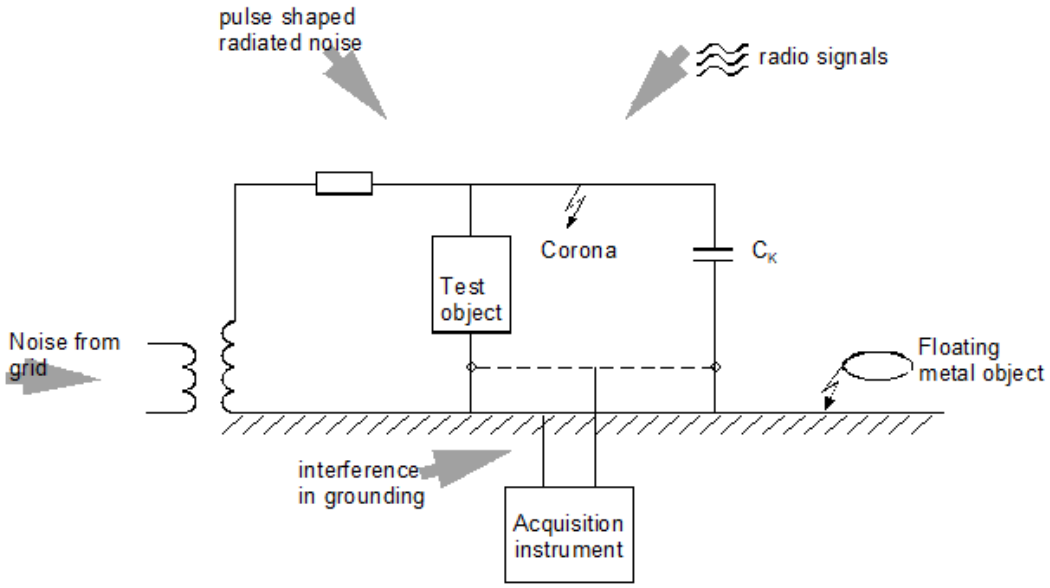

Figure 24: Most common sources of noise in the power grid [7].

For each optical measurement, the noise level was evaluated before performing PD measurements. The noise level is independent of the voltage level, which made it easier to recognize which signals were noise and which were actual PDs. However, the noise signals and dark currents overlapped some of the lower amplitude PDs, which made it challenging to recognize which signals were noise and which signals were PDs. As the noise level in the optical measurements typically had a maximum value of 1 a.u., the threshold value for defining what is considered a PD was set to 1 a.u. As the maximum PDs occurring had an amplitude of about 8.5 a.u., the range of PDs that was detected was between 1-8.5 a.u.

3.4.2 Test conditions

When analyzing the results that are collected in laboratory experiments, it is crucial to know about plausible sources of error in the data. This ensures that the results are precise, reproducible, and comparable with former and subsequent studies. Therefore, a big part of the laboratory work consisted of mitigating the impact of undesired PDs. Undesired PDs involve exaggerated PD formation due to metallic particles or

gas bubbles in the insulation. In addition, excessive PDs gathering around the zero crossing of the sinusoidal voltage would be interpreted as some unwanted error in the measurement system.

By being as consistent with the test procedure and test conditions as possible, any undesirable interference from noise or other sources of error could be assumed to be of similar magnitude for each test iteration. The pressboard and the dielectric liquid were renewed and vacuum treated properly before every measurement, to ensure that the insulation was not altered from the previous measurement and also so that no gas bubbles or particles were in the insulation. In addition, the insulation was visually inspected to see if the viscosity was normal and if any shiny metallic particles or other contaminations were present.

The brass electrodes were manufactured to be heavy enough to sufficiently flatten the pressboard. This was important, as one of the main problems Skribekk encountered in her work was that the pressboards were deformed after the drying process and therefore the pressboards were not completely flat during the measurements [13]. Another important measure was to properly clean the brass electrode by applying an ultrasonic cleaner to a box filled with isopropanol and keeping the electrode submerged in it. This ensured a successful removal of numerous tiny metallic particles that rested on the surface of the electrode. These metallic particles would have a detrimental effect on the accuracy of the measurements, as explained in section 2.5.

Between every measurement, the sharp electrode was treated very carefully to prevent any damaging deformations to its sharp edge. In addition, the electrode always had to be cleaned between each measurement due to gel formation around the edge of the electrode. This viscous gel was created due to many high-amplitude PDs from the previous measurement. It was observed that not removing this gel would result in fewer PD signals for a given voltage level. In the literature, this gel is often referred to as x-wax. The creation of x-wax in dielectric oil under electric stress has been shown to depend on temperature, moisture, and copper content, where the temperature influences the x-wax formation the most [29]. The formation and effects of x-wax/gel formation are further discussed in section 4.

3.4.3 Measurement procedure

Discharge probability and maximum PD amplitude as a function of the applied voltage were studied. The voltage was either a 30 Hz bipolar square voltage or a 30 Hz sinusoidal voltage. Each measurement was carried out by stressing the insulation for approximately 3 seconds and recording 50 of the voltage periods in this time span, for a given voltage level. The voltage was increased in steps of 1 kV to obtain sufficient data to make voltage-dependent plots. All PMT signals exceeding 1 a.u. were defined as a PD, which seldom included a small degree of unavoidable dark currents. As table 2 shows, 5 measurements were conducted on each insulation combination and voltage application. 5 measurements were performed to obtain average values and standard deviations.

Table 2: Number of measurements on each insulation combination and voltage application.

Dielectric liquid	Waveform	Rise time [ns]	PD detection	Number of measurements
Nytro 10XN	Bipolar	300	Positive	5
			Negative	5
		50	Positive	5
			Negative	5
	Sinusoidal	-	Positive	5
			Negative	5
Midel 7131	Bipolar	50	Positive	5
			Negative	5
	Sinusoidal	-	Positive	5
			Negative	5

Settings on the oscilloscope

With regards to the choice of sampling frequency and time window on the oscilloscope, it was set based on a trade-off between the resulting file size, the required time resolution for PD analysis, and when PDs typically occurred. For the tests performed with the Nytro-impregnated sample in the square voltage setup, the sampling frequency was set to 2.5 ns/point, which ensured a high resolution of the PD data collected. The time window was set to 40 μs, which meant that data were only recorded the first 40 μs of each voltage half-period. This was considered sufficient since the bulk of the discharges occurred in this time span for every voltage level. This is illustrated in figure 25, where it is clearly shown that all of the discharges can be observed in the first 40 μs of the voltage half-period.

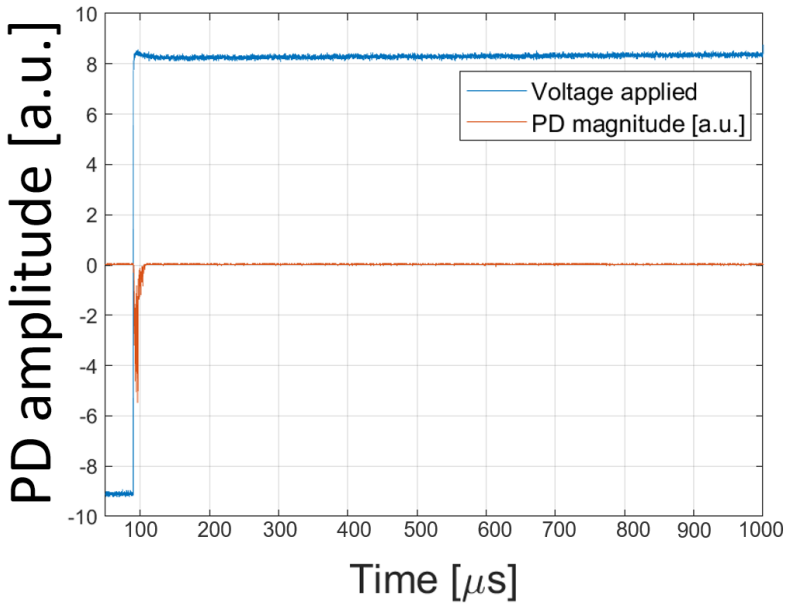

Figure 25: Typical discharge occurring the first 40 μs in a Nytro 10XN impregnated sample stressed by bipolar voltages.

In Midel however, the discharges often occurred later in a given voltage half-period compared to Nytro. So even though 40 μs was a sufficient time window for Nytro, the

time window had to increase to 1000 μs in Midel. Figure 26 shows a typical discharge in Midel occurring about 400 μs out in the voltage half-period. For the measurements performed in Midel, the sampling frequency was lowered to 80 ns/point to avoid generating exaggeratedly large data files. Unfortunately, this sampling frequency was later discovered to be too low in relation to the typical duration of a discharge in Midel. Partial discharge is a very transient phenomenon, and measurements actually showed that they typically last for about 10 ns. Thus, it became apparent that having the sampling frequency at 80 ns/point would mean that some critical information about the PDs will not get captured. This was a slight blunder in the measurements that was discovered too late to do the measurements over again.

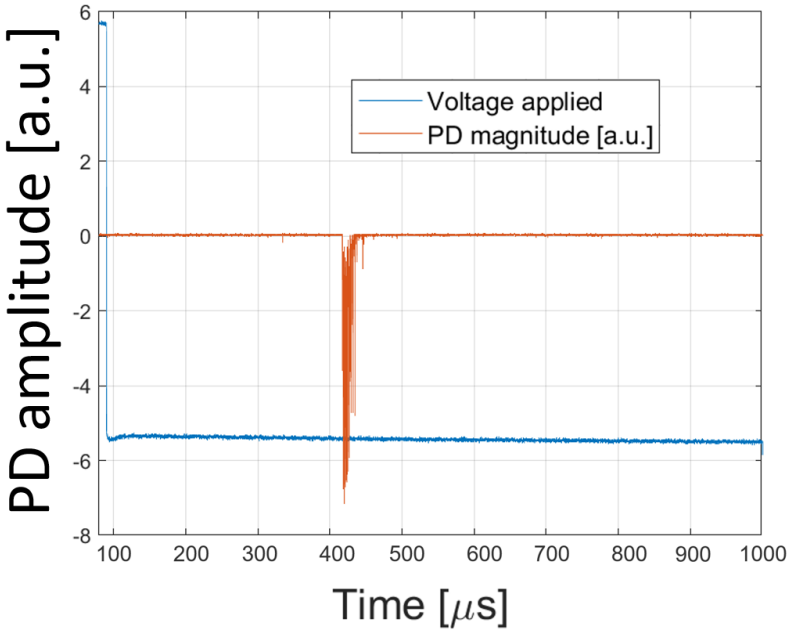

Figure 26: Typical discharge occurring the first 1000 μs in a Midel 7131 impregnated sample stressed by bipolar voltages.

When performing measurements in the sinusoidal voltage setup, experiments showed that the discharges could occur anywhere on a given voltage half-period. This meant that the whole half-period needed to get captured on the oscilloscope. The challenge then became apparent; how is it possible to capture all PD data with sufficient resolution without generating unfeasibly huge data files? That is when the setting called *Peak detect* was discovered in the oscilloscope manual [27].

Peak detect made it possible to capture all the peak values for a set acquisition interval, without generating too large files. This is in contrast to the setting that was used in the square voltage measurements, which were solely based on a setting called *Sample mode*. The differences between these two settings are illustrated in figure 27. With the setting *Peak detect*, this enabled a drastically lower sampling frequency of 2000 ns/pt, while still obtaining sufficient data to do systematic studies on discharge probability and maximum PD amplitude.

Acquisition mode	
Sample mode retains the first sampled point from each acquisition interval. Sample is the default mode. The instrument does no post processing of the acquired samples in this mode.	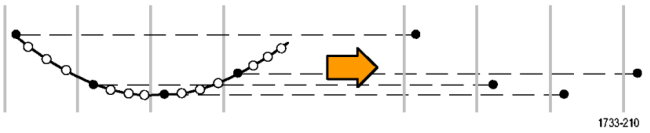
Peak Detect mode retains the highest and lowest values of all the samples in two consecutive acquisition intervals. This mode only works with real-time, noninterpolated sampling and is useful for catching high frequency glitches.	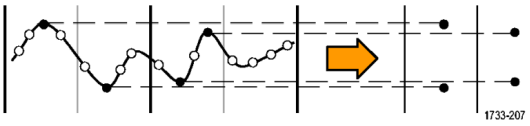

Figure 27: The difference between the acquisition modes *Sample mode* and *Peak detect*. Retrieved from the Tektronix oscilloscope manual [27].

Discharge probability and maximum PD amplitude

To measure the discharge probability for a given voltage level, it was counted how many of the total amount of half-periods (N_{pulses}) that contained PD signals ($N_{signals}$). The discharge probability was then calculated by taking the ratio of these two and multiplying it by 100%, as shown in equation 1. This means that for a given voltage half-period, a single discharge signal is enough to qualify as a contribution to $N_{signals}$ in equation 1. For the measurements performed in the laboratory, N_{pulses} was set to 100 for all voltage levels.

$$\text{Discharge probability} = \frac{N_{signals}}{N_{pulses}} \cdot 100\% \tag{1}$$

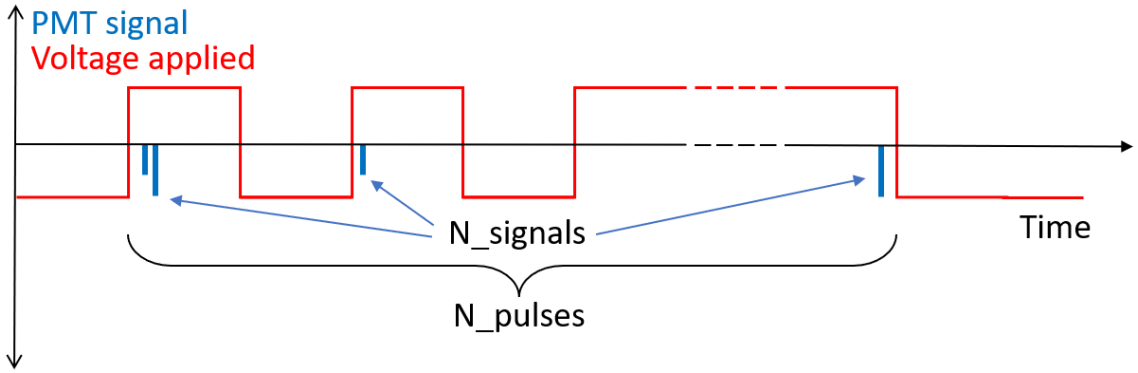

Figure 28: Demonstration of how discharge probability was obtained, based on $N_{signals}$ and N_{pulses}. Reproduced from [30].

The procedure for obtaining discharge probability curves was similar to what Folkestad did in her master's thesis in spring 2022, which partly served as an inspiration for how this section is built up [30].

The maximum PD amplitude was obtained by extracting the peak PMT signal of each measurement, i.e. the maximum PMT signal of all 100 voltage half-periods. The time at which the maximum PD amplitude occurred was also studied, as this was observed to be correlating with the higher voltage levels in Nytro. This was done

for all 5 measurements, and then the average values and standard deviations were calculated. Figure 29 illustrates what the maximum PD amplitude value and time represent for a given measurement.

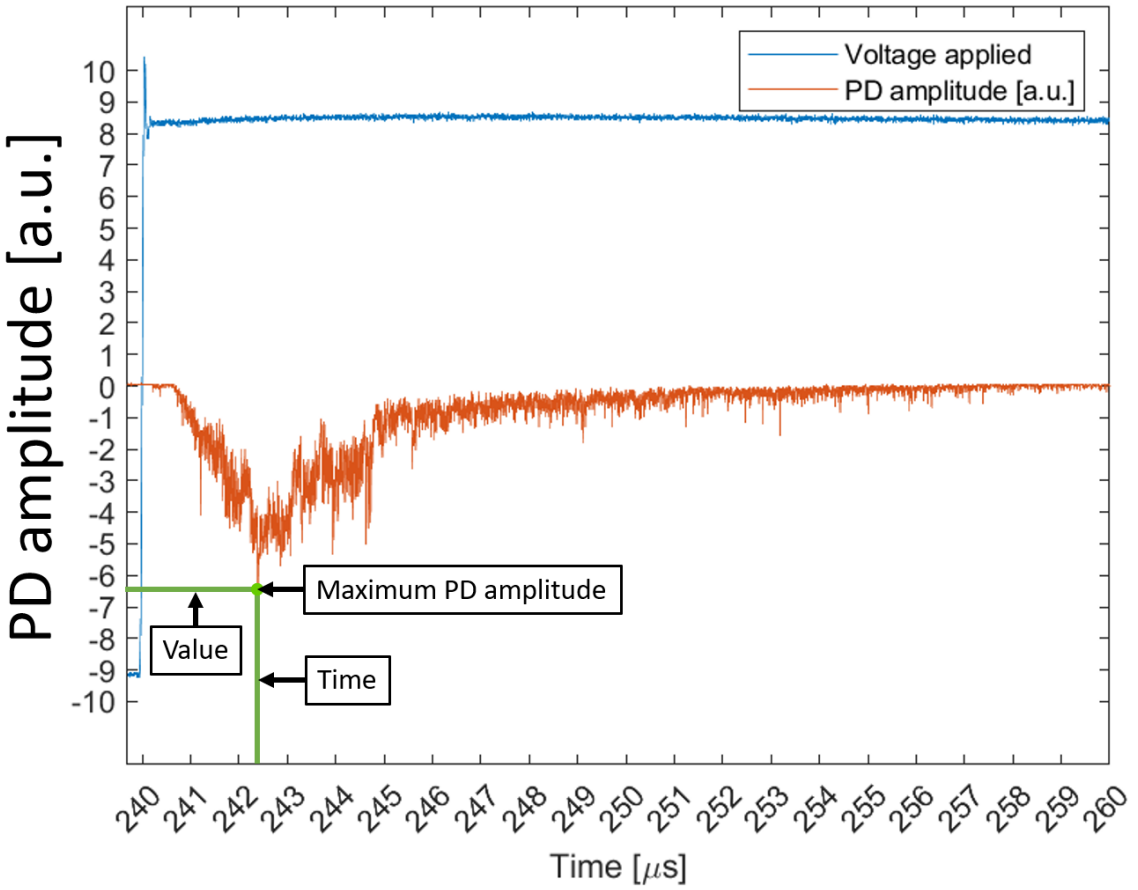

Figure 29: Typical PMT-signal (red) and applied voltage (blue). The maximum PD amplitude is indicated.

4 Results and discussion

The sections 4.1 and 4.2 show the results for the PD characteristics in Nytro and Midel, respectively. Both of these sections contain four subsections that deal with rise time variations, polarity differences, discharge pictures & oscillograms, and visible ageing of the pressboards.

For the subsections on rise time variations and polarity differences, the discharge probabilities and maximum PD amplitudes are presented. The method for obtaining discharge probability and maximum PD amplitude was thoroughly explained in section 3.4.3. Section 4.3 presents informative graphs to compare and summarize the results on discharge probability and maximum PD amplitude in Nytro and Midel. Finally, sections 4.4 and 4.5 discuss the influence of space charges and sources of error in the measurements, respectively.

4.1 PD characteristics of Nytro-impregnated pressboards

4.1.1 Rise time variations

As shown in figure 30, the discharge probability is clearly higher for lower rise times, for every given voltage level. This is in agreement with the earlier research on the topic, presented in section 2.6. The standard deviation is also quite small, which means that the results had great reproducibility. It is worth observing that the discharge probability for the bipolar square voltages increases rapidly from about 10% to 90% during only 4 voltage levels. In contrast, the discharge probability in the sinusoidal measurement increased very slowly and almost linearly from about 0% to 65% during 18 voltage levels.

The difference in the development of discharge probability as a function of the applied voltage can at least partly be explained by the degree of gel formation around the tip of the electrode. Since the gel formation is highly dependent on the applied voltage level, the slow and linear increase can be explained by the fact that the gel works as a protective shield against discharge formation. Pictures of the gel and further discussions on this are presented in section 4.1.4.

Another explanation for the differences between the sinusoidal and the square voltage measurements is the space charge effect, which earlier research has shown to be highly dependent on the duration of the applied voltage (as presented in section 2.3.1). As [4] puts it: "With short duration, fast rise-time impulses there is little time for charges to travel, while for ac and even dc the space charges have ample time to build up." Thus, it is likely that the space charge effect is more present for the sinusoidal measurements compared to the square voltage measurements.

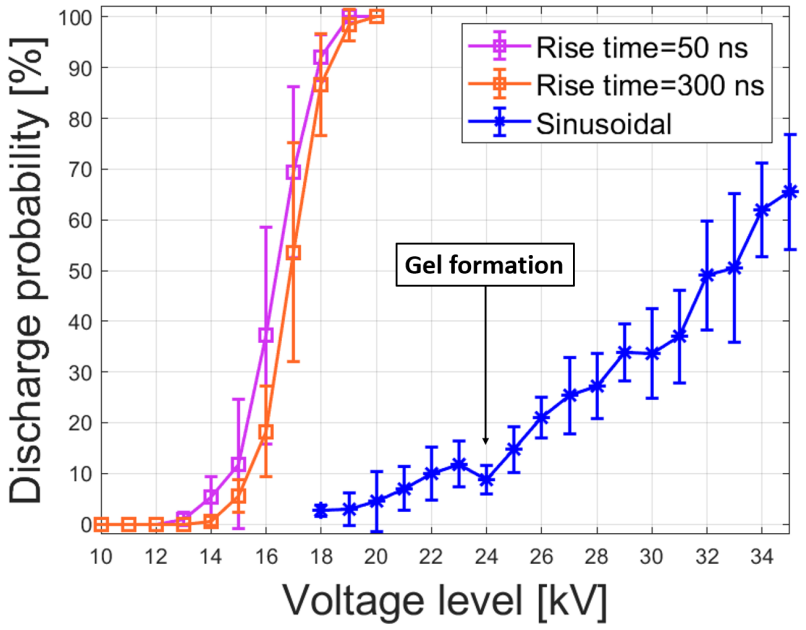

Figure 30: Discharge probability in Nytro, for three different voltage applications.

Figure 31 shows that the maximum PD amplitude is higher for lower rise times, for every given voltage level. This is also in agreement with the earlier research on the topic, presented in section 2.6. Compared to the discharge probability from figure 30, it is interesting to see that the maximum PD amplitude for the sinusoidal measurement increases at a much faster pace until about 25 kV. From 26 kV, however, the maximum PD amplitude increases very slowly for each voltage level. It is also worth noting that the standard deviation decreases significantly for higher maximum PD amplitudes. For instance, for maximum PD amplitudes exceeding 7 a.u. (arbitrary unit), the standard deviation is close to zero for all three voltage applications.

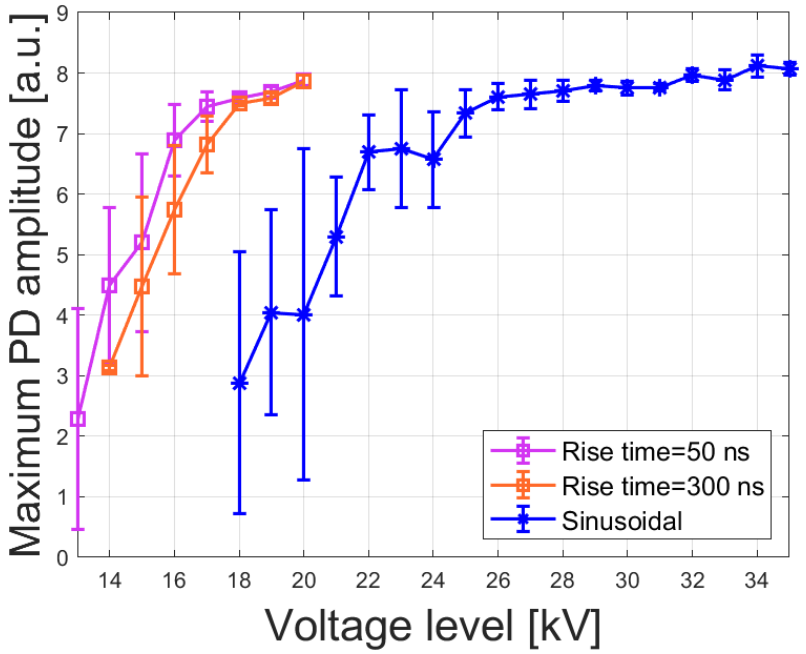

Figure 31: Maximum PD amplitude for the Nytro-impregnated insulation system, for three different voltage applications.

Figure 32 shows the maximum PD amplitudes and the time at which they occur in relation to the applied voltage. The two voltage waveforms on the top of the figure illustrate two different rise times of the applied voltage. The horizontal and vertical standard deviation at each point illustrates the standard deviation for time and maximum PD amplitude, respectively. Recall that the maximum PD amplitude and time are average values from 5 measurements and the method for obtaining the values are presented in section 3.4.3. As can be seen, for higher voltages and higher maximum PD amplitudes, the discharges seem to occur earlier in relation to the applied voltage. In addition, the results suggest that for a rise time of 50 ns, the maximum PD amplitudes occur earlier than those for a rise time of 300 ns. However, since the average differences are relatively small and the standard deviations overlap considerably, these findings do not suffice as evidence.

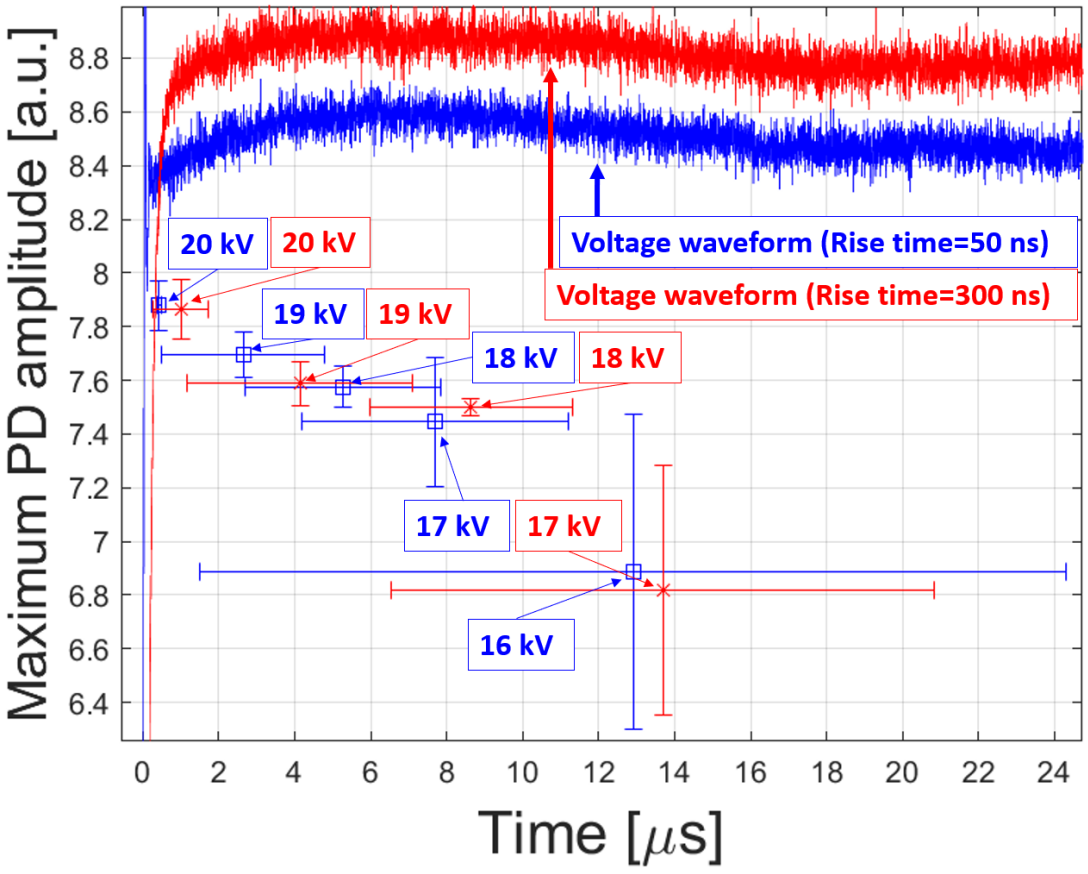

Figure 32: Maximum PD amplitude in Nytro, for two different rise times. Horizontal and vertical standard deviations are included.

4.1.2 Polarity differences

Figure 33 shows that for bipolar square voltages, the positive polarity discharges have lower discharge probability for every voltage level, compared to the negative polarity discharges. Interestingly, the results on the sinusoidal voltages show the opposite trend, namely that the negative polarity discharges are significantly higher compared to the positive polarity discharges. The difference between the polarities in the sinusoidal measurement generally increases for every voltage level. This is in agreement with the results on PD repetition rate from the preceding project [14], as

presented in section 2.4.

The increasing polarity difference in discharge probability for the sinusoidal measurement is suspected to correlate to the degree of gel formation on the pressboard, see section 4.1.4. The space charge effect was presented in section 2.3.1 and could be a plausible explanation for how the gel amplifies these polarity differences. This is because the gel could make it easier for space charges in form of slow-moving positive ions to get trapped in the gel. This could then be creating a lower resulting electric field (called Poisson field) around the tip of the electrode for the positive polarity voltages, and thus explains the relatively low positive discharge probability for the sinusoidal measurement. Conversely, when the tip is negative, this will cause a lower discharge probability and thus could explain the relatively high discharge probability for the sinusoidal measurement.

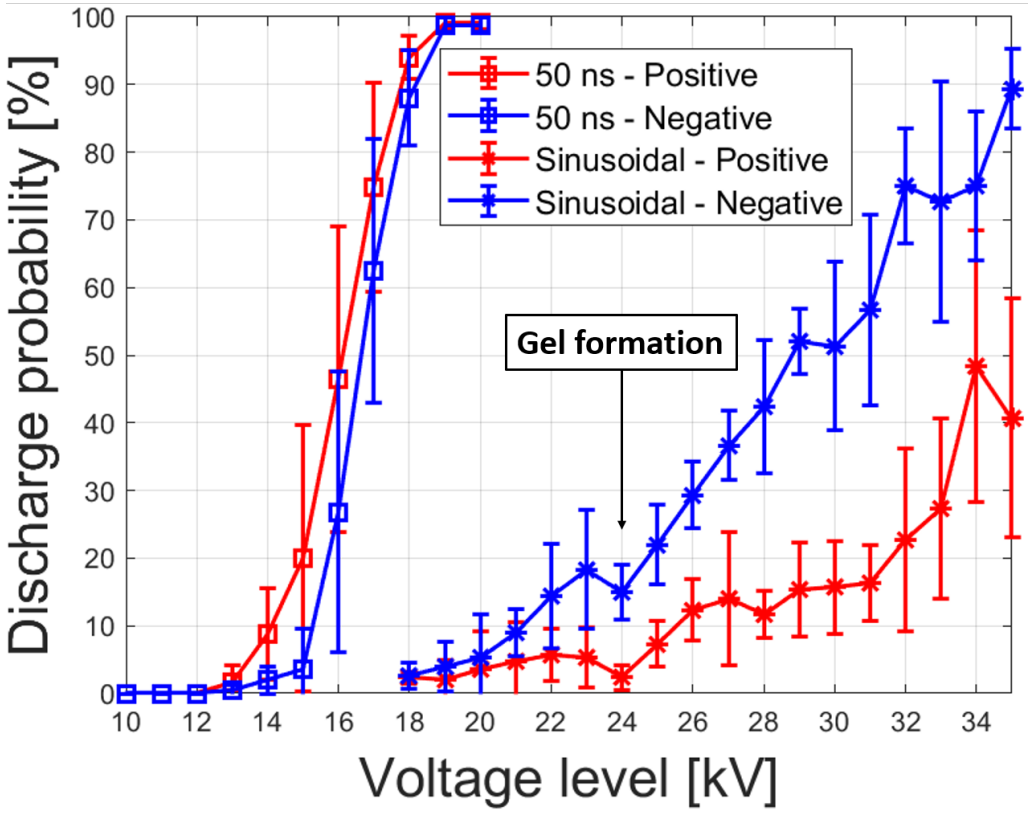

Figure 33: Discharge probability for the Nytro-impregnated insulation system, for square and sinusoidal measurements for both polarities.

Figure 34 shows the maximum PD amplitude for the square and sinusoidal voltage measurements, for both polarities. It can be seen that there are only small average differences and big overlaps in the standard deviations for the two polarities. Therefore it seems that there are no clear polarity differences to be observed in terms of maximum PD amplitude in Nytro. This is a bit unexpected, considering that earlier research on positive polarity streamers has shown to have higher maximum PD amplitudes than negative polarity streamers, for the same applied voltage [5].

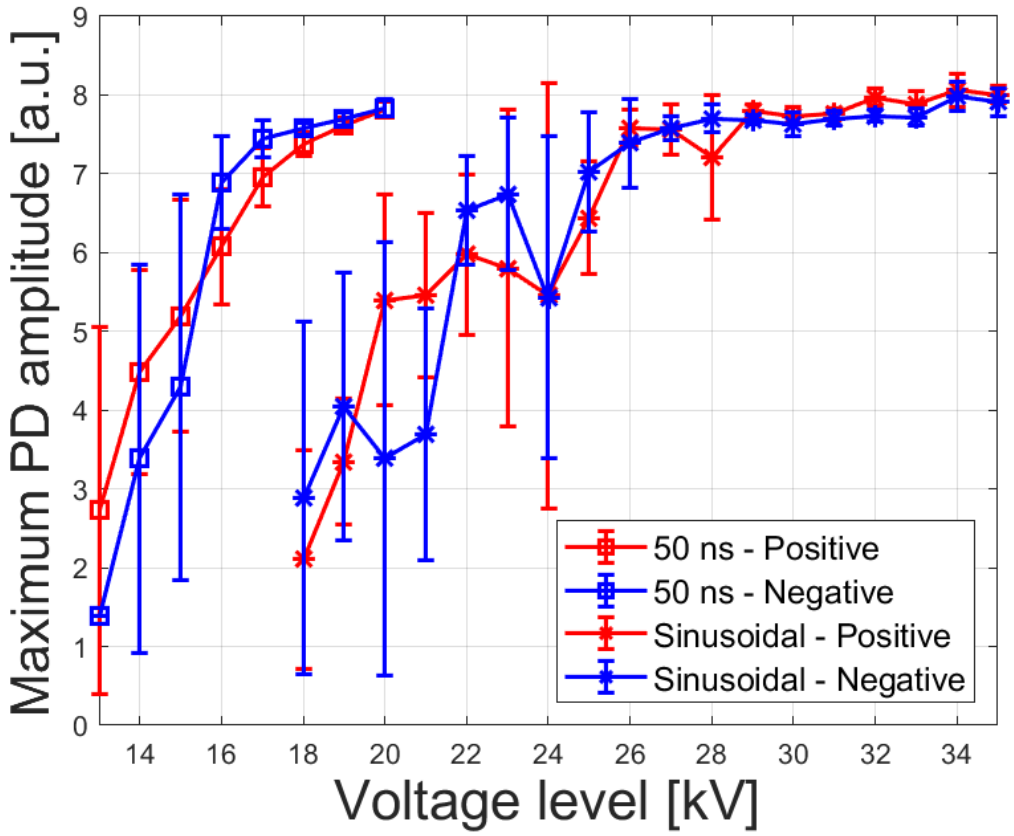

Figure 34: Maximum PD amplitude for the Nytro-impregnated insulation system, for square and sinusoidal measurements for both polarities.

4.1.3 Pictures and oscillograms

Figure 35 illustrates the result from one measurement in Nytro, stressed by 1000 bipolar square voltage half-periods at 16 kV, with a rise time of 300 ns. The big, solid yellow circle represents the electrode and each small circle point on its circumference represents the location of discharges that have occurred during the measurement. The color of the small circle points indicates the polarity of the first discharge on that specific location, where red means positive polarity and blue means negative polarity. The solid red square on the bottom of the electrode is a reference for the placement of the electrode, which is the same as for the measurement performed in Midel in section 4.2.3.

Each number inside the different white brackets represents the half-period number at which a discharge has occurred, in the range from 0 to 1000. Similar to the small circle points, the color of the numbers indicates the polarity of the discharge of that voltage half-period number. As bipolar square voltage half-periods are applied, this naturally implies that even and odd half-period numbers will be of opposite polarity. In the case illustrated in figure 35, the odd numbers are positive polarity discharges and the even numbers are negative polarity discharges.

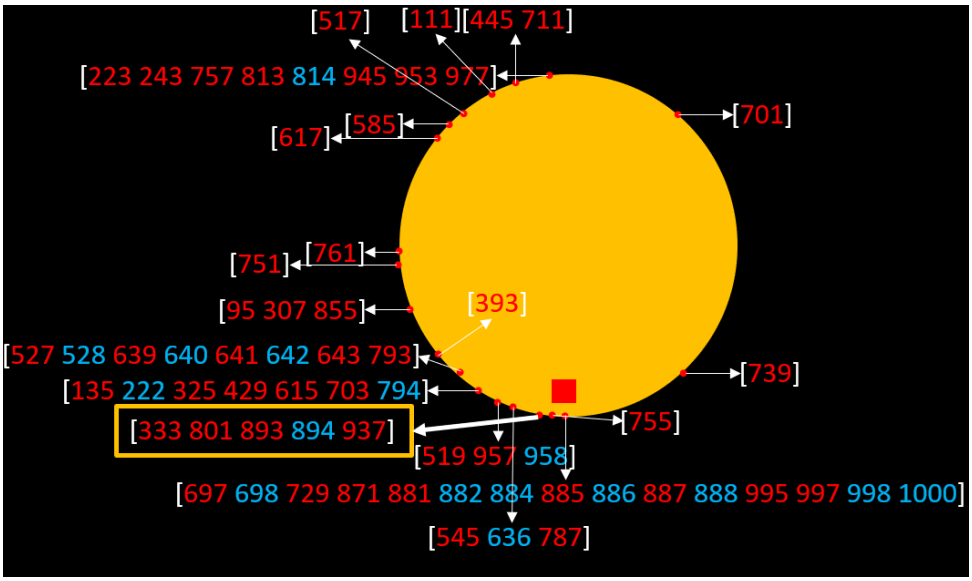

Figure 35: Location and half-period number of all discharges occurring when stressed by 1000 bipolar square voltage half-periods at 16 kV in Nytro. Red number: Positive polarity discharge. Blue number: Negative polarity discharge.

As seen, every single first discharge on a new location on the electrode is initiated on a positive voltage half-period. In addition, when a negative polarity discharge appears, it is often after a positive polarity discharge has occurred in the preceding voltage half-period. For this measurement, $\frac{7}{12} \cdot 100\% = 58.3\%$ of the negative polarity discharges occurred this way. Another interesting observation is the fact that the bulk of the discharges occurred on the left side of the electrode. This could mean that the probability of initiating a discharge on a location is higher if a discharge already has occurred close by.

It is also important to notice that even though discharges often occur in consecutive periods on a specific location, it is just as often tens or even hundreds of half-periods between each discharge occurrence on a given location. This is illustrated more clearly in the histogram in figure 36, where the number of half-periods between two consecutive discharges on a location and the respective number of occurrences is illustrated. For instance, as can be seen in the figure, about 33.9% of the total amount of discharges occurred one half-period after the preceding discharge (n=1). At n=100 a thicker pillar is shown to represent all half-periods between 100 and 1000, which are 32.6% of the total amount of discharges. This indicates that there is a certain memory effect in the insulation.

A reason for the memory effect in Nytro is its high field conductivity, which is found to be very high compared to Midel [31]. Due to this, the time constant for ions and electrons is relatively low and thus the lifetime of a discharge is not very long. This could help explain why there are no discharges on n=3 and n=4 in Nytro.

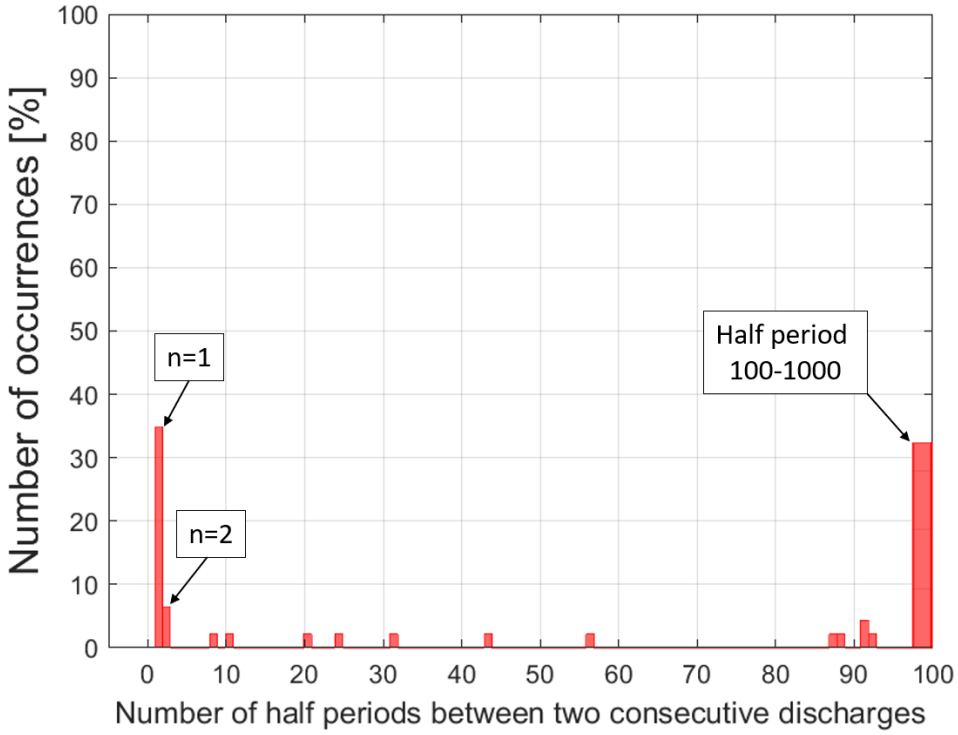

Figure 36: Histogram illustrating the number of half-periods between two consecutive discharges. This is from one measurement in Nytro stressed by 1000 bipolar square voltage half-periods at 16 kV, with a rise time of 300 ns.

In figure 35 above, the half-period numbers 333, 801, 893, 894, and 937 are placed inside a yellow rectangle. These specific discharges are studied in greater detail in figure 37a-37e, where pictures of the discharges along with the corresponding oscillogram are shown. In addition, the length of each discharge is indicated in the pictures of the discharges.

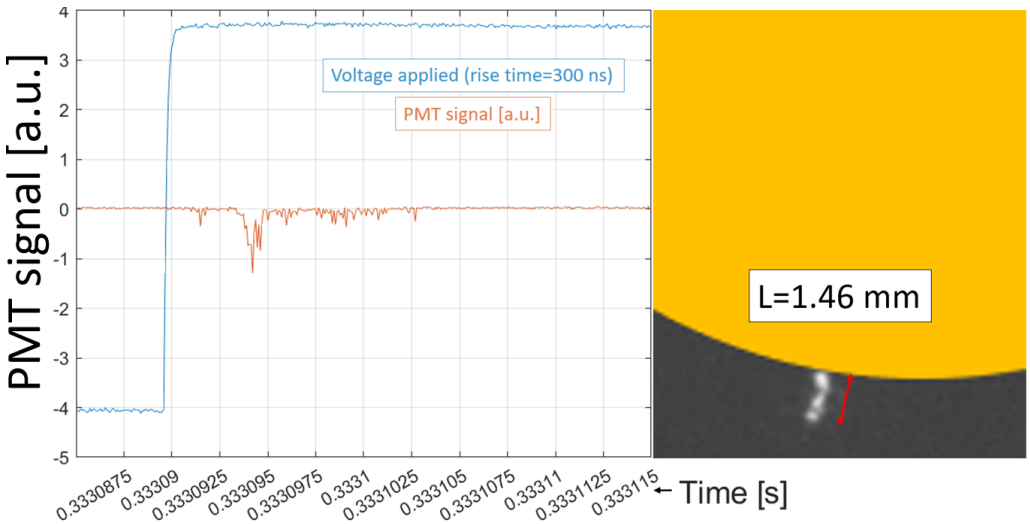

(a) Positive polarity discharge at voltage half-period number 333/1000.

Figure 37: Oscillograms and pictures of discharges occurring on the same location during a measurement with 1000 bipolar voltage half-periods. Rise time=300 ns (Continues on next page).

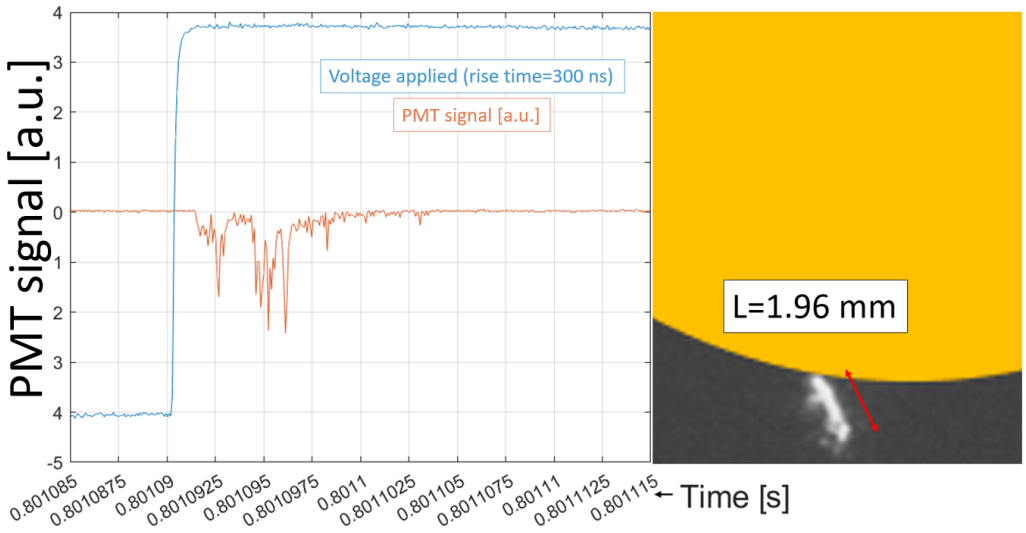

(b) Positive polarity discharge at voltage half-period number 801/1000.

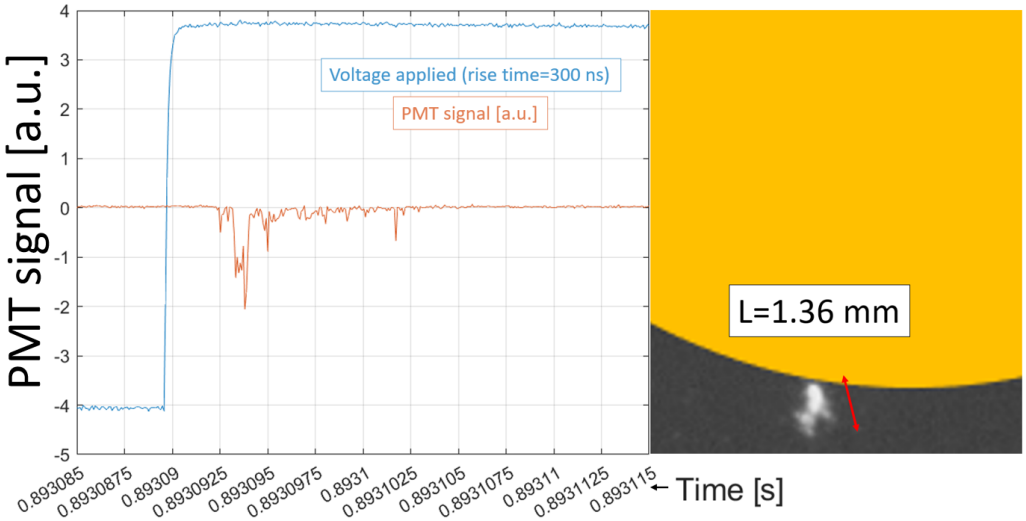

(c) Positive polarity discharge at voltage half-period number 893/1000.

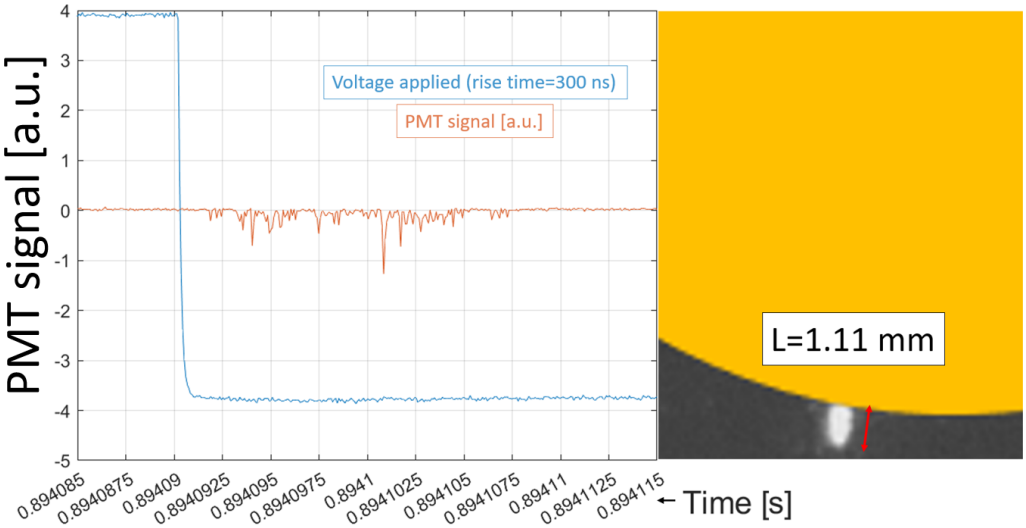

(d) Negative polarity discharge at voltage half-period number 894/1000.

Figure 37: Oscillograms and pictures of discharges occurring on the same location during a measurement with 1000 bipolar voltage half-periods. Rise time=300 ns (Continues on next page).

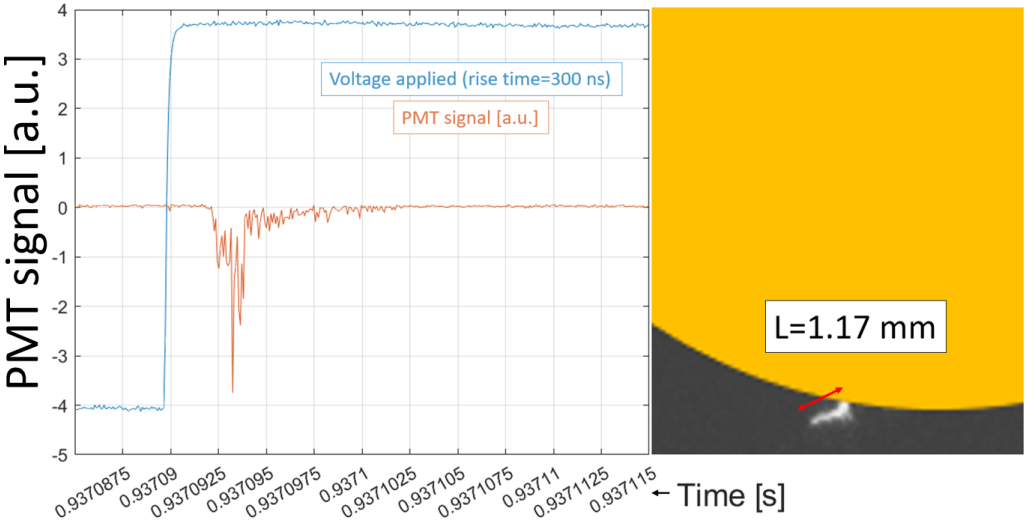

(e) Positive polarity discharge at voltage half-period number 937/1000.

Figure 37: Oscillograms and pictures of discharges occurring on the same location during a measurement with 1000 bipolar voltage half-periods. Rise time=300 ns.

4.1.4 Visible ageing of the insulation

Figure 38 and 39 shows the gel that has formed on the surface of the pressboard after a bipolar square voltage measurement (t_r=300 ns) and sinusoidal voltage measurement, respectively. As can be seen, the amount of gel is significantly larger in the sinusoidal measurement. The amount of gel was observed to correlate to the size and the number of discharges that occurred on the pressboard during the measurement. Since the sinusoidal voltage measurement had larger discharges due to the high applied voltage, it follows that there is significantly more gel on this pressboard compared to the square voltage measurement. The gel was observed to function as a protective shield against discharges in the measurements. This could help explain why the discharge probability in the sinusoidal measurement in figure 30 increased so slowly for the higher voltages. It could also be the reason why the polarity differences were so distinct in figure 33. This is because the gel could make it easier for space charges in form of slow-moving positive ions to get trapped and thus create a lower resulting electric field around the tip of the electrode for the positive polarity voltages.

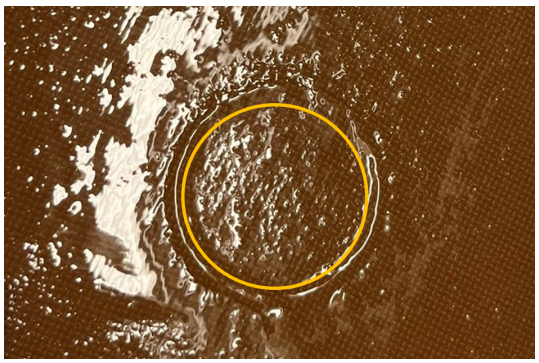

Figure 38: Gel formation in Nytro, after a square voltage measurement up to 20 kV. Electrode location is indicated.

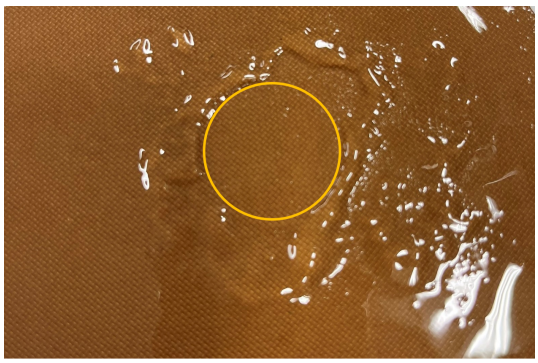

Figure 39: Gel formation in Nytro, after a sinusoidal voltage measurement up to 35 kV. Electrode location is indicated.

4.2 PD characteristics of Midel-impregnated pressboards

4.2.1 Rise time variations

Figure 40 shows the discharge probability for the bipolar square voltage and sinusoidal voltage measurement in Midel. Similar to Nytro, the discharge probability is much higher for the square voltage measurement compared to the sinusoidal voltage measurement. However, the standard deviation is quite high on several of the voltage levels, which makes the results less reproducible. For both voltage stresses, the discharge probability increases almost linearly after exceeding 10% discharge probability.

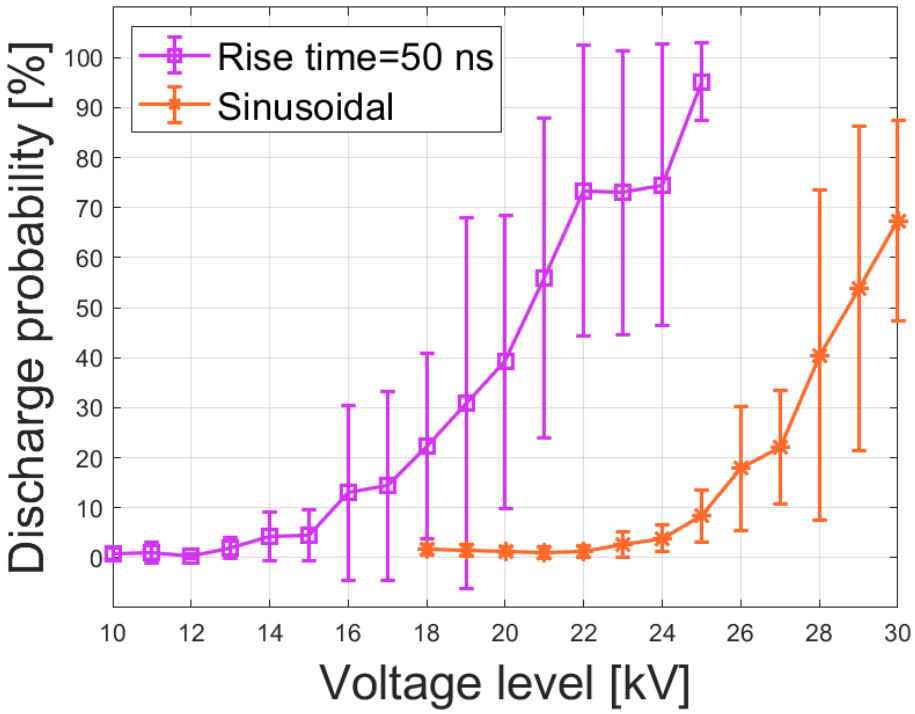

Figure 40: Discharge probability for the Midel-impregnated insulation system, for square and sinusoidal voltages.

The maximum PD amplitude presented in figure 41 is higher for lower rise times, for every given voltage level. However, there are big standard deviations for several of the early voltage levels in the sinusoidal and square voltage measurements. Here it is important to remember the discharge probability measurement from figure 40. This is because when the discharge probability is low, it follows that large average differences in the maximum PD amplitude will occur. For the sinusoidal voltage measurement, the first few voltage levels might seem peculiar at first glance. Especially at 20 kV, where the standard deviation is zero and the maximum PD amplitude is about 1 a.u. This is in line with the discharge probability from figure 40, where it can be seen that the discharge probability is almost zero between 18 kV and 22 kV, and doesn't exceed 10% before 26 kV. Thus, the explanation for the standard deviation being zero at 20 kV is simply that only one discharge occurred at this voltage level for all of the 5 measurements.

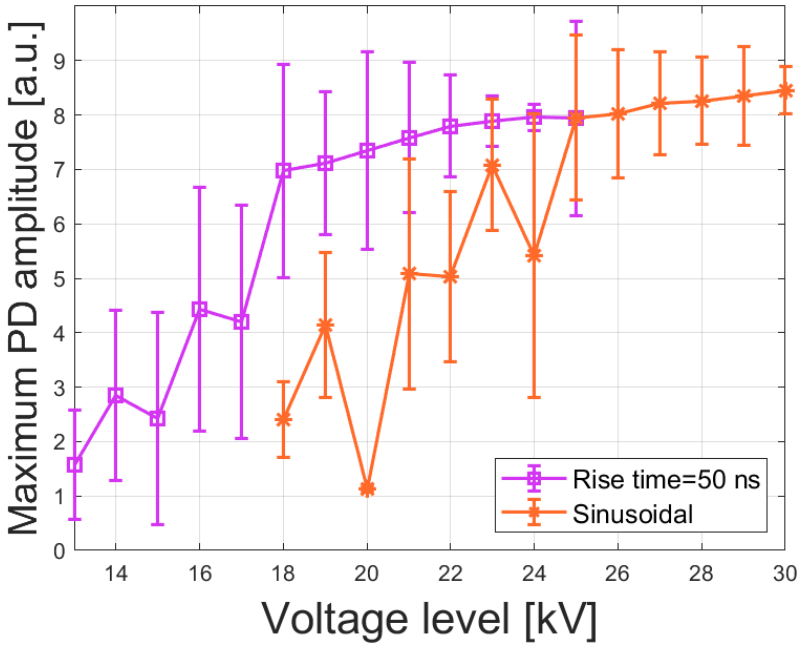

Figure 41: Maximum PD amplitude for the Midel-impregnated insulation system, for square and sinusoidal voltages.

Figure 42 shows the maximum PD amplitude and where on the voltage curve it occurred on average. In contrast to the Nytro result presented in figure 32, there seems to be no clear correlation between the maximum PD amplitude and where it occurs in relation to the applied voltage. Also, the standard deviations are very large for all voltage levels except 25 kV. However, the maximum PD amplitudes on voltage levels 22 kV to 25 kV seem to be clustering close to the rising edge of the applied voltage. It is worth recalling from section 3.4.3 that the discharges in Midel generally occurred anywhere between 0 and 1000 μs out in a given voltage half-period.

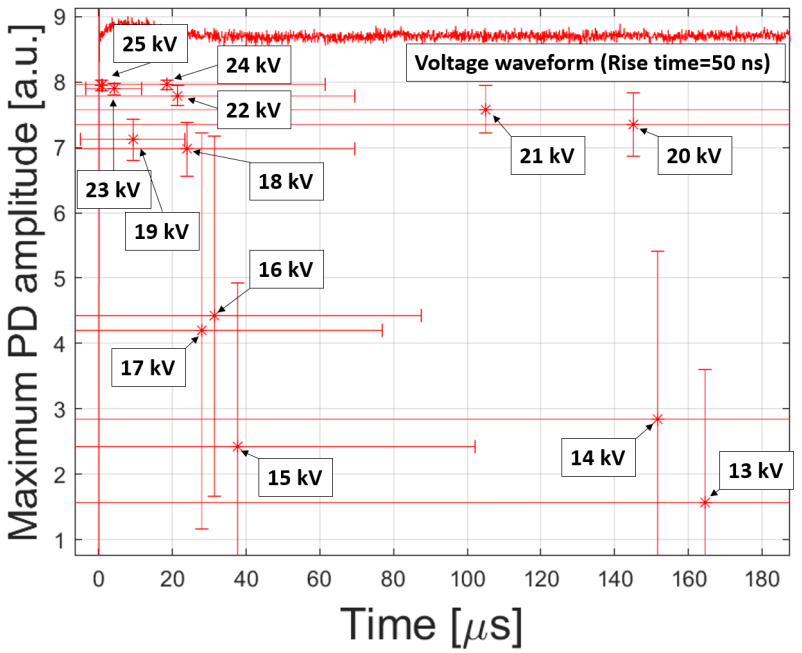

Figure 42: Maximum PD amplitude for the Midel-impregnated insulation system, for square voltages with a rise time of 50 ns.

4.2.2 Polarity differences

Figure 43 shows that for both the square and sinusoidal voltage measurements, the positive polarity discharges generally have higher discharge probability for every voltage level. The difference is largest for the square voltage measurement between 16 kV and 20 kV and the standard deviations are quite high. However, compared to Nytro, the polarity differences of discharge probability are much smaller in Midel, especially for the sinusoidal measurement. For the sinusoidal measurement in Nytro, the negative polarity discharge probability was much higher than the positive polarity discharge probability. Since almost no gel was formed in the Midel measurements (see section 4.2.4), this supports the explanation for the polarity differences in Nytro. To more easily compare the discharge probability in Nytro and Midel, see figure 50 in section 4.3.

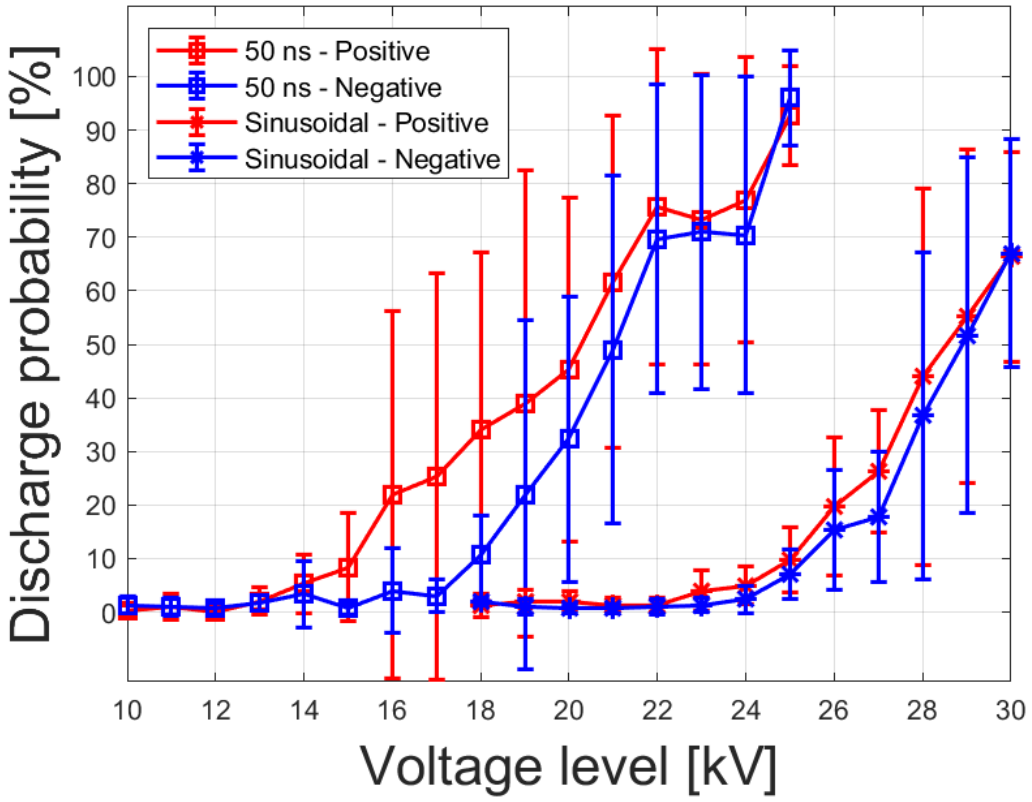

Figure 43: Discharge probability for the Midel-impregnated insulation system, for both polarities and two different voltage applications.

Figure 44 shows the maximum PD amplitude in Midel for the square and sinusoidal measurement, for both polarities. The standard deviations were left out because their large size created too much chaos in the plot. The general shape of the curves can be recognized from figure 41, which presented the same result but without separating the polarities. As can be seen in figure 44, the maximum PD amplitudes for the positive polarity are bigger than the negative polarity, for every voltage level, just like in Nytro. Also, the maximum PD amplitude for the sinusoidal measurement is very large for the highest voltage levels in Midel. Because of these large discharges, the measurement had to be stopped at 30 kV to avoid dielectric breakdown of the insulation. To more easily compare the maximum PD amplitude in Nytro and Midel, see figure 51 in section 4.3.

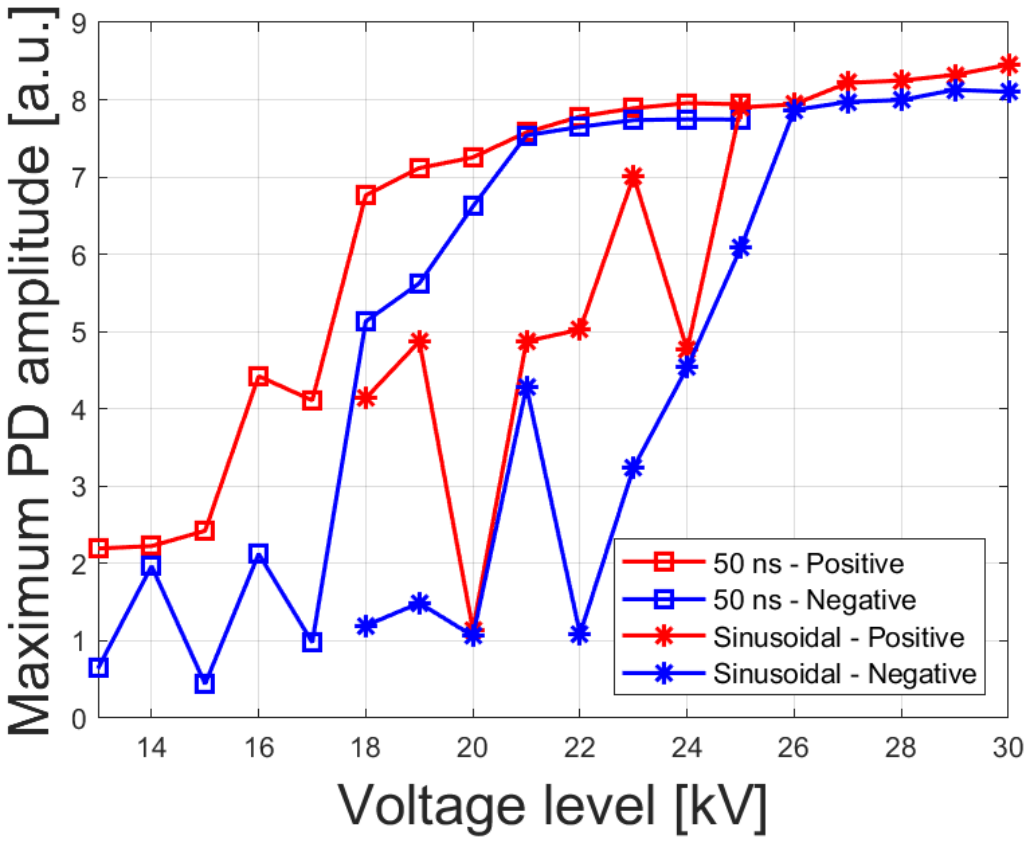

Figure 44: Maximum PD amplitude of the Midel-impregnated insulation system, for both polarities and for square and sinusoidal voltages.

4.2.3 Pictures and oscillograms

Figure 45 shows the results from one measurement in Midel stressed by 1000 bipolar square voltage half-periods at 23 kV, with a rise time of 300 ns. As can be seen, the bulk of the discharges occurred on the right side of the electrode. This is in contrast to the measurement performed in Nytro, where almost all the discharges appeared on the left side of the electrode. Recall that the solid red square on the bottom of the electrode is a reference for the positioning of the electrode.

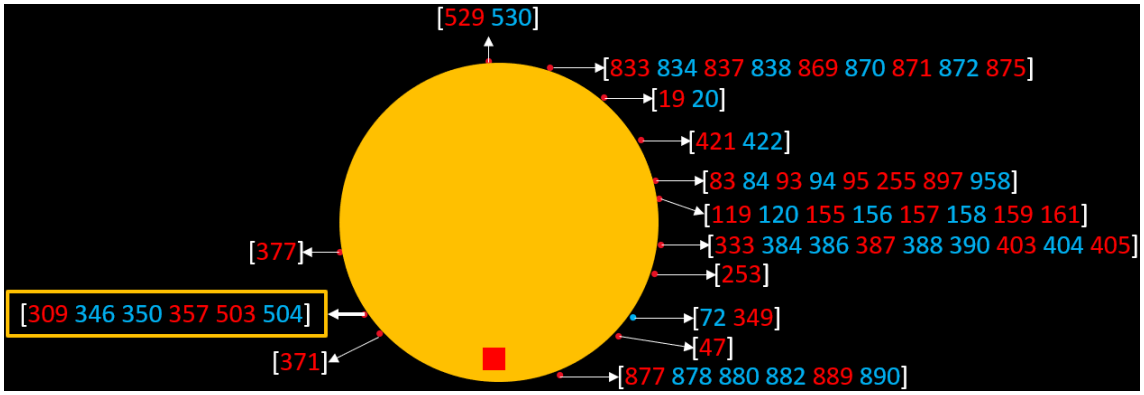

Figure 45: Location of discharges occurring when stressed by 1000 bipolar square voltage half-periods at 23 kV in Midel. Red numbers: Positive polarity discharge. Blue numbers: Negative polarity discharge.

It can be seen that similar to Nytro, every first discharge (except half-period number 72) on a new location on the electrode is initiated on a positive voltage half-period. Also, when a negative polarity discharge appears, it is in $\frac{17}{26} \cdot 100\% = 65.4\%$ of the cases after a positive polarity discharge has occurred in the preceding voltage half-period.

Compared to Nytro, there generally seem to be fewer half-periods between each following discharge on a given location in Midel. For instance, in Nytro it was often several hundred half-periods between each discharge on a location, but in Midel this was much rarer. This is illustrated more clearly in the histogram in figure 46, where the number of half-periods between two consecutive discharges and the respective number of occurrences are illustrated. This points to a lesser memory effect in Midel compared to Nytro.

Another relevant fact to consider is the high field conductivity of Midel, which is found to be very low compared to Nytro [31]. The time constant for the discharge is relatively high and thus the lifetime of a discharge is longer compared to Nytro. This could help explain why there are discharges on n=3 and n=4.

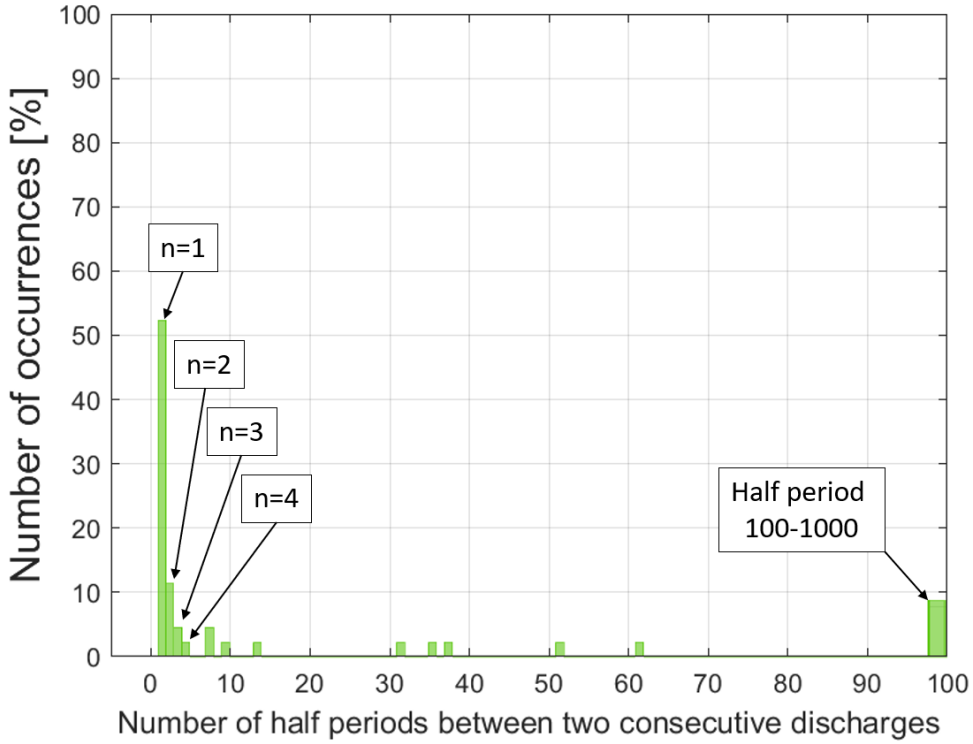

Figure 46: Histogram illustrating the number of half-periods between two consecutive discharges. This is from one measurement in Midel stressed by 1000 bipolar square voltage half-periods at 23 kV, with a rise time of 300 ns.

In figure 45 above, the half-period numbers 309, 346, 350, 357, 503, and 504 are placed inside a yellow rectangle. These specific discharges are studied in greater detail in figure 47a-47f, where pictures of the discharges along with the corresponding oscillogram are shown. In addition, the length of each discharge is indicated in the pictures of the discharges.

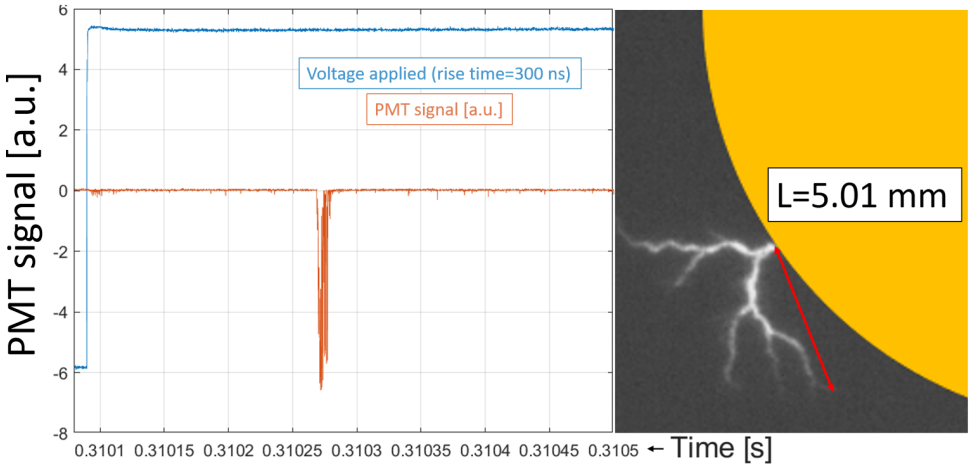

(a) Positive polarity discharge at voltage half-period number 309/1000.

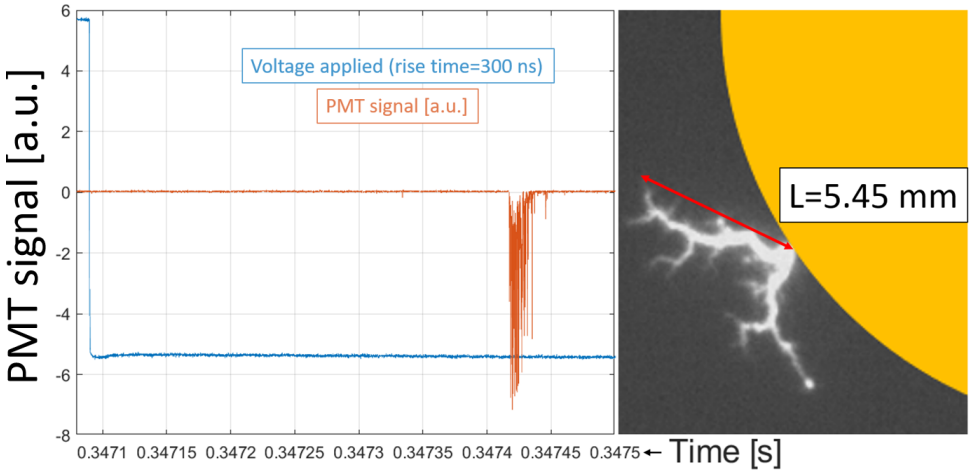

(b) Negative polarity discharge at voltage half-period number 346/1000.

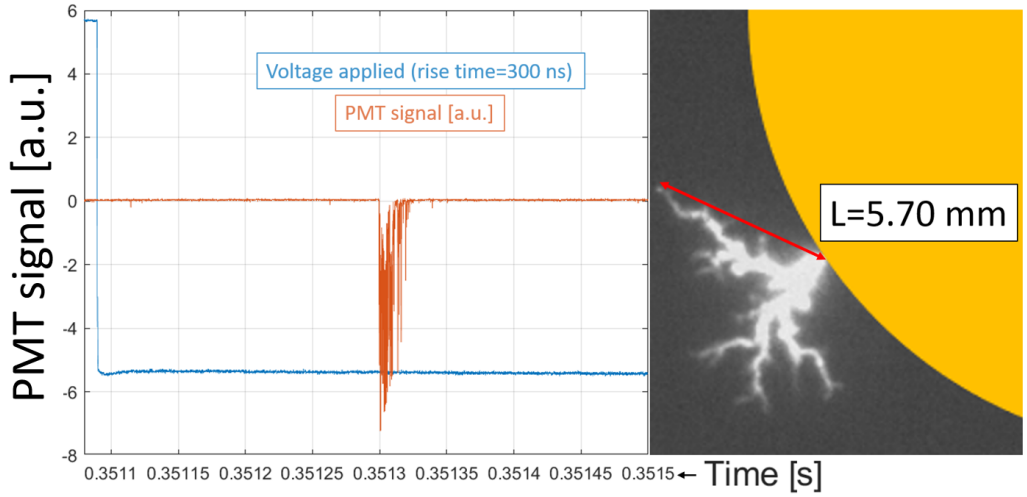

(c) Negative polarity discharge at voltage half-period number 350/1000.

Figure 47: Oscillograms and pictures of discharges occurring on the same location during a measurement with 1000 bipolar voltage half-periods (Continues on next page). Rise time=300 ns.

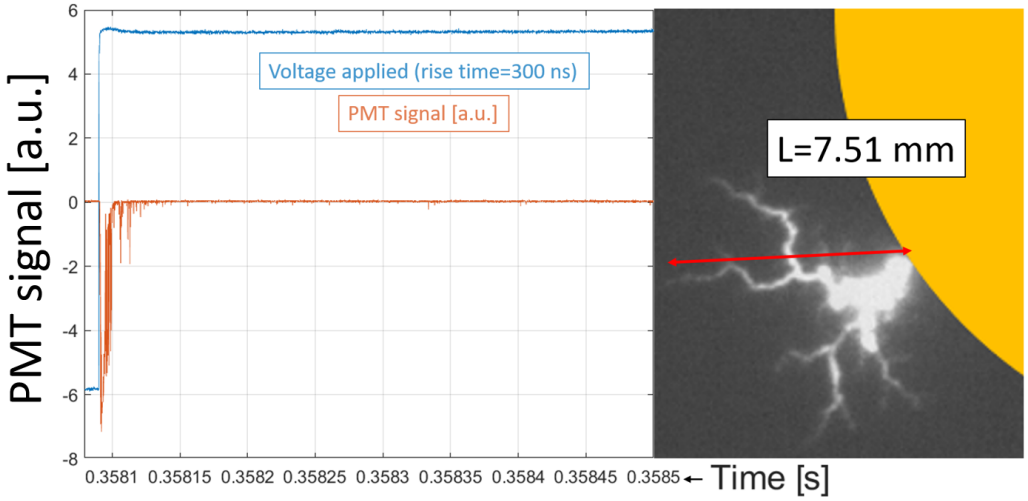

(d) Positive polarity discharge at voltage half-period number 357/1000.

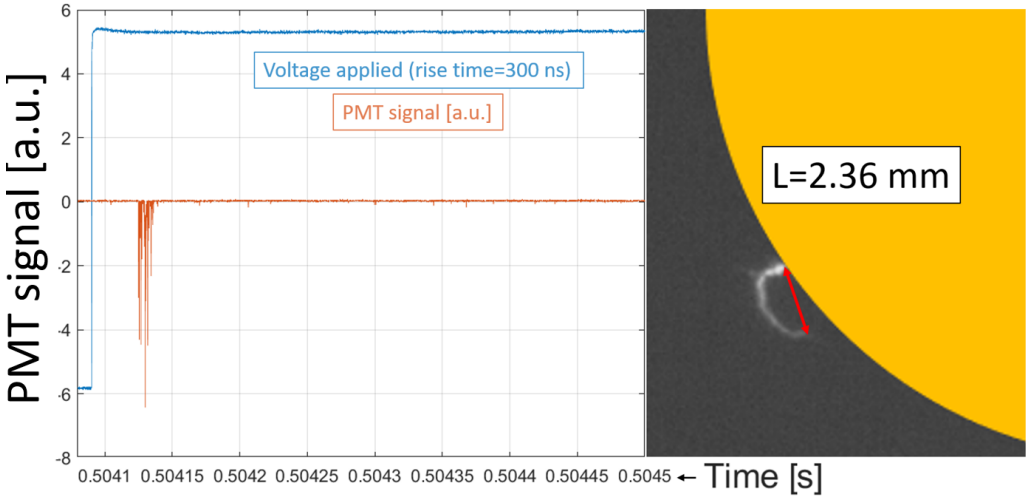

(e) Positive polarity discharge at voltage half-period number 503/1000.

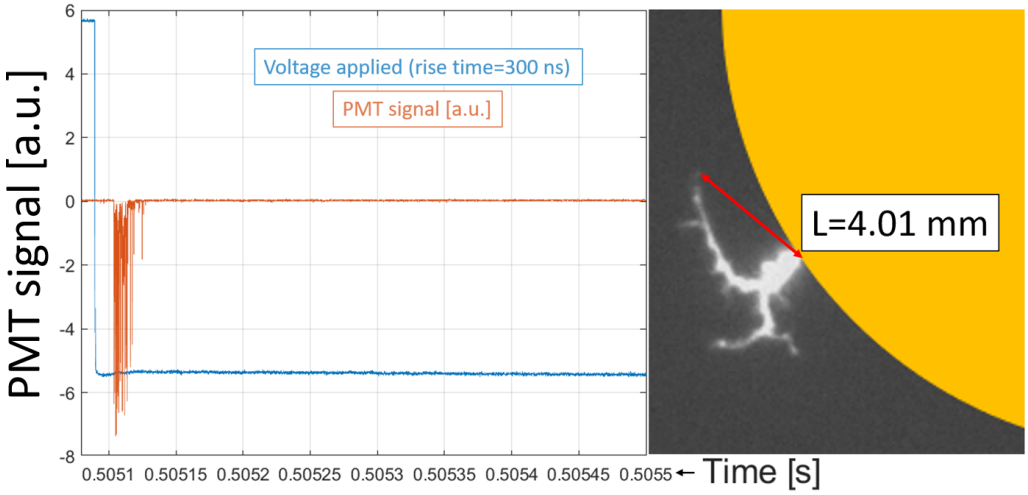

(f) Negative polarity discharge at voltage half-period number 504/1000.

Figure 47: Oscillograms and pictures of discharges occurring on the same location during a measurement with 1000 bipolar voltage half-periods.

4.2.4 Visible ageing of the insulation

Figure 48 and 49 show the small amount of gel that was formed on the surface of the pressboard after a square voltage and sinusoidal voltage measurement, respectively. As seen, the amount of gel is barely visible in both measurements and is thus considered to have a minimal effect on the discharge initiation and propagation.

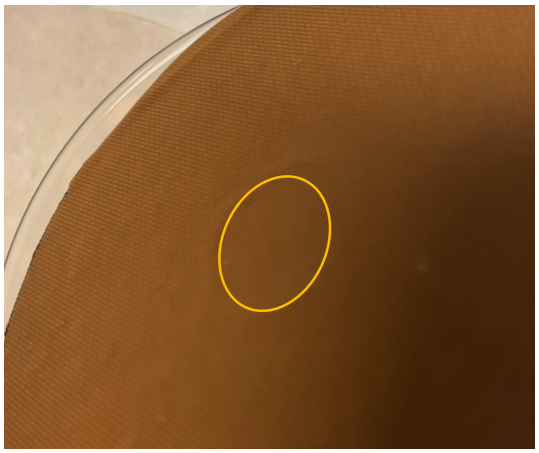

Figure 48: Small amounts of gel in Midel, after a bipolar voltage measurement up to 25 kV with rise time=50 ns. Electrode location is indicated.

Figure 49: Small amounts of gel formation in Midel, after a sinusoidal voltage measurement up to 30 kV. Electrode location is indicated.

4.3 Comparative PD characteristics of Nytro and Midel

Figure 50 shows an overview of the discharge probabilities in Midel and Nytro for both polarities in the square and sinusoidal voltage measurements. To read the plots and compare the different results, its worth mentioning that the red and green graphs represent the results for Nytro and Midel, respectively. Also, the dark and light color of red and green indicates positive and negative polarity results, respectively. Finally, the square and star data points are made to differentiate between square and sinusoidal voltage measurements.

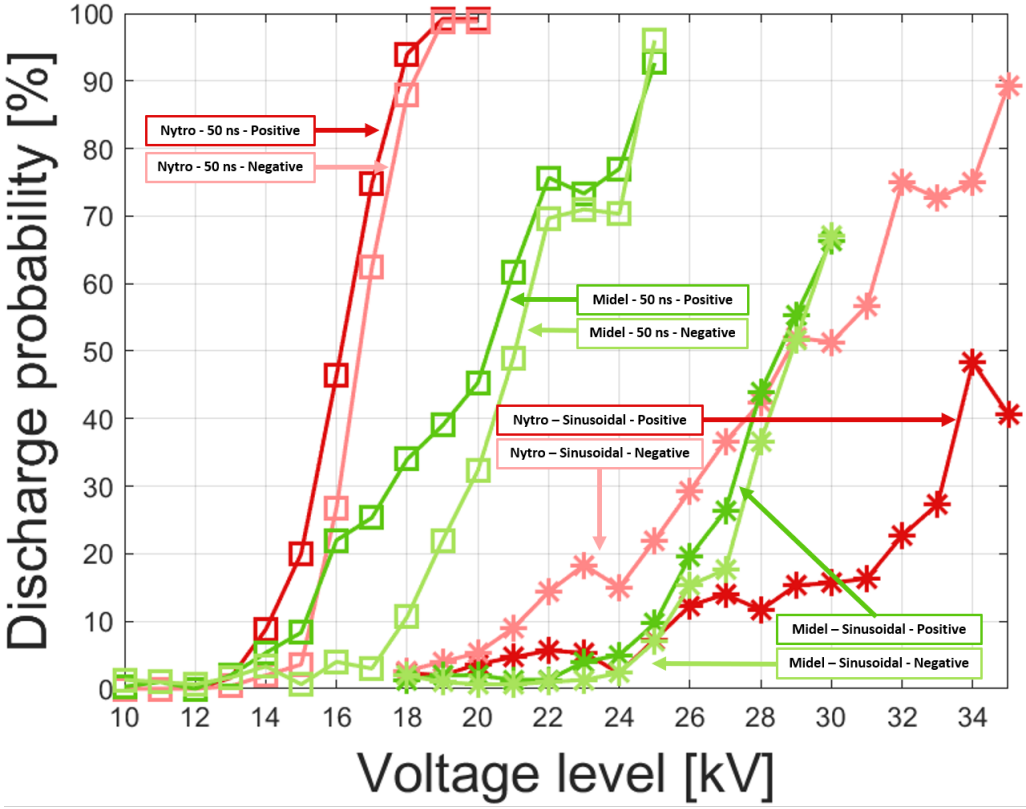

Figure 50: Discharge probability for the insulation systems impregnated by Nytro and Midel.

For the square voltage measurements shown in figure 50, Nytro and Midel are quite similar with regard to polarity differences. However, the graphs clearly show that Nytro generally has a higher discharge probability for every voltage level compared to Midel. The discharge probability also increases at a much faster pace in Nytro compared to Midel.

For the sinusoidal measurements, however, there are big differences between Nytro and Midel both in terms of polarity differences and overall discharge probability. For Nytro, the negative polarity discharge probability is 2-3 times as big as the positive polarity. In contrast, Midel has a relatively similar development for the polarities, where the positive polarity discharge probability is slightly larger than the negative polarity discharge probability for every voltage level. The large difference in gel formation in Nytro and Midel is expected to be the main explanation for this. Further, it can be seen that Midel has a lower discharge probability than Nytro up to about 28 kV, where it exceeds Nytro.

Figure 51 shows the maximum PD amplitude for the sinusoidal and square voltage measurements in Nytro and Midel. The polarity differences were left out because they were not significant. As can be seen, the maximum PD amplitude in Nytro is consistently higher for the square voltage measurements compared to Midel. For the sinusoidal measurement, however, there are no clear differences to be observed before 25 kV has been reached. From this voltage level, the maximum PD amplitude in Midel is higher than in Nytro for the rest of the measured voltage levels. Due to the large discharges in Midel, the measurement had to be stopped at 30 kV to avoid dielectric breakdown of the insulation. In Nytro however, it was possible to increase the voltage up to 35 kV. This seems to imply that the withstand capability of Nytro is larger than in Midel. However, recall again that the gel is assumed to influence the results in Nytro considerably.

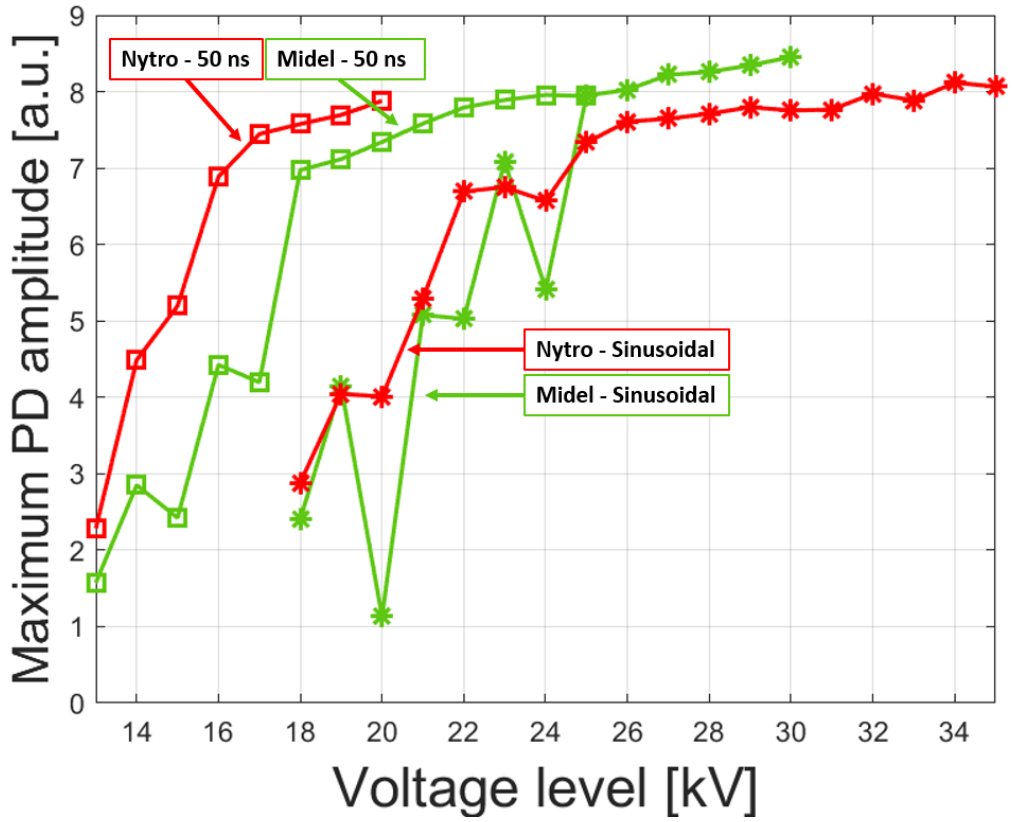

Figure 51: Maximum PD amplitude for the insulation systems impregnated by Nytro and Midel.

4.4 Space charge effect

There were big differences in discharge probability and maximum PD amplitude for the square and sinusoidal measurements. A probable explanation for these differences is the space charge effect, which earlier research has shown to be highly dependent on the duration of the applied voltage (as presented in section 2.3.1). A shorter voltage duration gives a shorter time for charge emission from the electrode, while sinusoidal voltages provide much more time for the space charges to develop [4]. This makes it likely that the space charge effect is more present for the sinusoidal measurements compared to the square voltage measurements.

The escalating polarity difference in discharge probability for the sinusoidal measurement in Nytro is suspected to correlate to the degree of gel formation on the pressboard, see section 4.1.4. The space charge effect is assumed to explain how the gel contributes to these polarity differences. This is because the gel could make space charges in the form of slow-moving positive ions get trapped in the gel. This will then produce a lower resulting electric field around the tip of the electrode for the positive polarity voltages. The Poisson field is thus created and the effect shown in the orange line in figure 52 is present. This figure only shows the case for a positive anode, but when the anode is negative, this will cause a lower discharge probability for the negative polarity voltages. Hence, this could explain the larger discharge probability for the negative polarity compared to the positive polarity for the sinusoidal measurements in Nytro.

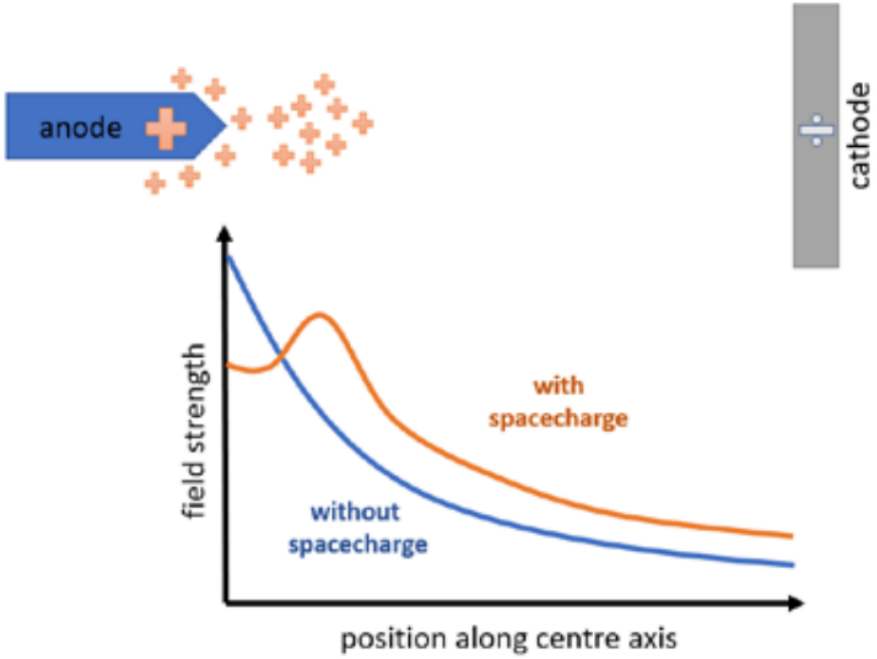

Figure 52: The effect of space charges in a needle to plane arrangement [4].

4.5 Sources of error

There are numerous parameters that could have influenced both the accuracy and credibility of the results obtained. Considering the time limitations and practical feasibility, several improvements to the technical measuring procedures and changes to the test setup had to remain unexamined. The variables that could have influenced the results the most are listed in the following two sections.

4.5.1 Test object

- Damages to the edges of the electrode. The edges of the electrode could potentially get less sharp for each test iteration. A small change in electrode sharpness could affect the results significantly, as is confirmed by [10]. However, as the electrode was treated very carefully, no clear deterioration occurred on the electrode, and thus is considered to have a negligible influence on the result.

- Slight differences in the moisture content of the dielectric liquid and the pressboard. Some of the pressboards were made in separate batches, meaning that not all pressboards were dried and impregnated at the same time. Small changes in moisture content could cause noticeable changes in the obtained results [28]. Fortunately, the moisture content in both Nytro and Midel was measured to be approximately 0.4% for all batches, which implies that the results should be sufficiently comparable.
- Having an electrode with too low weight, causing a too low or uneven contact force between the sharp-edged electrode and the pressboard is a potential problem. This would make it more difficult to equalize the conditions for every test measurement. This did not appear to be a problem for the measurements, as the visual inspection of the test object indicated that the weight was sufficient. However, as the pictures of the discharges in section 4.1.3 and 4.2.3 revealed, there appeared to be a tendency for the discharges to occur on either the left or right side of the electrode. This could hypothetically be explained by an uneven contact force between the electrode and the pressboard. A more probable explanation, however, is that the probability of initiating a discharge at a specific location is higher if a discharge already has occurred close by.
- As presented in section 4, large discharges occurring during the measurements were observed to lead to gel formation on the pressboard in the Nytro measurements. This change in chemical composition and viscosity, unfortunately, made the results from the sinusoidal measurements in Nytro less comparable to the rest of the measurements, since there was far less gel formation in the other measurements. Since the gel had a shielding effect, a possible improvement to more accurately study the discharges as a function of the applied voltage would be to renew the test object for each voltage level increment.

4.5.2 Measurement procedure

- The procedure for obtaining PD results optically was not complying with any well-established measurement standard (such as IEC 60270 for electrical measurements). Hence, the results may not be displaying values that are analogous to the apparent charge that would be measured electrically. Especially when looking at the maximum PD amplitude, it is important to recall that the optical amplitude is not calibrated to any electrical value of the PD, and thus may be giving a misguided impression of the results. A considerable effort was put into trying to calibrate the electrical measurements to the optical measurements in the sinusoidal setup, but unfortunately, this was not successful. However, though the relative values may not be precise, the overarching trend is assumed to be credible.
- A thorough study of the properties of the PMT was not performed, and may thus be a source of error for the optical measurements.
- When extracting the maximum PD amplitude optically, it is debatable whether the procedure used in this thesis gives the most valuable information. Recall from section 3.4.3 that the maximum PD amplitude was obtained by extracting the peak PMT signal from each measurement consisting of 50 voltage periods. This means that the extracted value from a measurement is only based on one data

point. However, a PD contains several data points depending on the sampling frequency, and it could be reasonable to include the neighboring data points of the maximum value when determining the maximum PD amplitude. Another option would be to instead look at the sum of all the light signals for each voltage half-period, i.e. taking the integral of the PMT signals and thus giving an insight into the total amount of light emitted from the discharge. A final option would be to extract the maximum PD amplitude from every single voltage half-period and take the average of all of the obtained values.

5 Conclusion

Two types of dielectric liquids were used in the experimental tests to study PD characteristics. The first is the mineral oil Nytro 10XN and the second is the biodegradable synthetic ester Midel 7131. With this insulation system, the discharges were investigated by applying voltage to a sharp-edged electrode. A predefined number of 30 Hz bipolar square voltage pulses with varying rise times was applied for each voltage level, with voltage values ranging from 8 kV to 25 kV. In addition, it was performed tests with 30 Hz sinusoidal voltages ranging from 18 kV to 35 kV.

The discharge probability and maximum PD amplitude were higher for lower rise times, for every given voltage level in both dielectrics. A likely explanation for the rise time dependency of discharge occurrences is the space charge effect, which earlier research has shown to be highly dependent on the duration of the applied voltage. A shorter voltage duration gives a shorter time for the charges to emit from the electrode, while sinusoidal voltages provide much more time for the space charges to develop.

Further, the positive polarity discharge probability was generally higher compared to the negative polarity discharges in both dielectrics, except for the sinusoidal measurements in Nytro, where the negative polarity discharge probability was significantly higher compared to the positive polarity. In Nytro, a viscous gel would form during every measurement, where the amount of gel correlated with the size and the number of discharges that occurred during the measurement. The gel was observed to function as a protective shield against discharges in the measurements. This is suspected to be the reason why the polarity differences were so significant in the sinusoidal measurements in Nytro. That is because the gel could make it easier for space charges in form of slow-moving positive ions to get trapped and thus creating a lower equivalent electric field around the tip of the electrode for the positive polarity voltages.

The maximum PD amplitude in Nytro was higher than Midel for all the square voltage measurements. In the sinusoidal measurement, there were no clear differences until 25 kV was reached. From 25 kV the maximum PD amplitude in Midel was consistently higher than in Nytro for the sinusoidal measurement. The results indicate that for higher maximum PD amplitudes, the discharges occur on average earlier in relation to the applied voltage. Also, the results in Nytro suggest that for shorter rise times (t_r=50 ns), the maximum PD amplitudes occur earlier compared to those for longer rise times (t_r=300 ns). However, since the average differences were relatively small and the standard deviations overlapped a lot, these findings did not suffice as evidence.

Finally, a more in-depth analysis of discharges occurring in Nytro (16 kV) and Midel (23 kV) was performed. The results showed that every first discharge (except one in Midel) on a new location on the electrode in both dielectrics was initiated on the positive half-cycle of the voltage. When a negative polarity discharge appeared, it was in 58.8% (Midel) and 65.4% (Nytro) of the cases after a positive polarity discharge had occurred in the preceding half-period of the voltage. There were generally fewer half periods between each following discharge on a specific location in Midel compared to Nytro. This confirms that Nytro is more prone to the space charge effect

6 Suggestions for further work

This thesis has investigated how high-voltage insulation materials are affected by fast repetitive square voltage pulses compared to sinusoidal voltages. In addition, the insulation performance of the dielectric liquids Nytro 10XN and Midel 7131 were studied and compared. With hindsight, several parameters that would be interesting to study more in-depth became apparent. Therefore, some suggestions for further work are presented in the following bullet points.

- Adjust physical parameters such as pressboard thickness, moisture content, and electrode geometry and see how this affects the results.
- Perform measurements adjusting the parameters of the applied voltage, such as the rise time, switching frequency, duty cycle, voltage duration, and polarity.
- Do a systematic investigation on how the gel is formed in the dielectric liquid and how it affects the performance of the insulation. Perform measurements where the test object is renewed for every voltage level and compare this to measurements where it is not renewed. This will clearly show the effect of gel formation.
- Calibrate the optical measurements to the electrical measurements in the square voltage setup to obtain more realistic discharge magnitudes for the results gathered with the PMT, as done in [21].
- Perform a more in-depth analysis of the probability of consecutive discharges on a specific location on the electrode and see how the polarity, applied voltage, and dielectric liquid affects the results.
- Take pictures of discharges and make correlations between streamer length, applied voltage, discharge magnitude, polarity, their branching, etc.

References

[1] I. Khan and S. M. Muyeen. *Application of Power Electronics Converters in Smart Grids and Renewable Energy Systems*. July 2022.

[2] M. Roser and E. Ortiz-Ospina. Renewable energy. Published online at OurWorldInData.org. Retrieved from: 'https://ourworldindata.org/renewable-energy' [Online Resource]. 2022.

[3] M. Ghassemi. *Accelerated insulation aging due to fast, repetitive voltages: A review identifying challenges and future research needs*. Vol. 26. 5. 2019, pp. 1558–1568. DOI: 10.1109/TDEI.2019.008176.

[4] L. Lundgaard et. al. Dielectric performance of insulating liquids for transformers. Technical report, CIGRE, 2021.

[5] E. Ildstad. TET4160 - High voltage insulation materials. Technical report, NTNU, Department of Electric Power Engineering, 2021.

[6] A. Nysveen. TET4195 High voltage equipment - Power transformers. Technical report, NTNU, Department of Electric Power Engineering, 2015.

[7] L. Lundgaard. Partial Discharges - General Description. Technical report, SINTEF Energy Research, 2018.

[8] RCA Corporation. *Photomultiplier manual*. 1970.

[9] J. Quinn, L. Hrebien and Leonid. 'Development of a pattern recognition approach for analyzing flow cytometric data.' In: (Oct. 2022).

[10] X. Wang. *Partial discharge behaviours and breakdown mechanisms of ester transformer liquids under AC stress*. Ph.D Thesis, The University of Manchester, 2011.

[11] X. Zhou et al. *Study of Oil/Pressboard Creeping Discharges Under Divergent AC Voltage—Part III: Effects of Temperature and Stress Type*. Vol. 29. no. 1. 2022, pp. 119–126.

[12] X. Zhou et al. *Study of Oil/Pressboard Creeping Discharges under Divergent AC Voltage—Part 1: Fundamental Phenomena and Influencing Factors*. Vol. 28. no. 2. 2021, pp. 355–363.

[13] F. Skirbekk. *Transformer insulation stressed by power converters*. Master's Thesis, Department of Electric Power Engineering, NTNU, 2021.

[14] B. Fagerli. *AC voltage stress on transformer insulation materials*. Specialization project, Norwegian University of Science and Technology, 2022.

[15] T. Grav and L. Lundgaard. 'Currents in AC stressed liquid insulated needle plane gap'. In: *2014 IEEE 18th International Conference on Dielectric Liquids (ICDL)*. 2014, pp. 1–5. DOI: 10.1109/ICDL.2014.6893091.

[16] V. H. Dang et al. *Comparative PD characteristics of pressboard/mineral oil and pressboard/vegetable oil insulating systems*. 2012, pp. 890–893.

[17] 'From personal communication with post doctoral fellow Ivan Semenov (at the department of electric power engineering at NTNU).' In: 2022.

[18] CIGRE Working Group A2-35. Experiences in service with new insulating liquids. Technical report, CIGRE, 2010.

[19] M. Krins, H. Borsi and E. Gockenbach. *Influence of carbon particles on the breakdown and partial discharge inception voltage of aged mineral based transformer oil*. 1996, pp. 251–254.

[20] W.P. Robbins N. Mohan M. Undeland. Power Electronics: Converters, Applications, and Design. 3rd Edition. 2003.

[21] A. A. Abdelmalik, A. Nysveen and L. Lundgaard. *Influence of fast rise voltage and pressure on partial discharges in liquid embedded power electronics*. Vol. 22. 5. 2015, pp. 2770–2779. DOI: 10.1109/TDEI.2015.005411.

[22] P. Wang, A. Cavallini and G. C. Montanari. 'Characteristics of PD under square wave voltages and their influence on motor insulation endurance'. In: *IEEE Transactions on Dielectrics and Electrical Insulation* 22.6 (2015), pp. 3079–3086. DOI: 10.1109/TDEI.2015.005158.

[23] B. Florkowska et al. 'Measurement and analysis of surface partial discharges at semi-square voltage waveforms'. In: *IEEE Transactions on Dielectrics and Electrical Insulation* 18.4 (2011), pp. 990–996. DOI: 10.1109/TDEI.2011.5976086.

[24] B. M. Notaros. Electromagnetics. Department of Electrical and Computer Engineering at Colorado State University, 2011.

[25] I. Semenov et al. 'Characterization of defects in aluminum nitride substrates through partial discharge measurements'. In: *2022 IEEE 4th International Conference on Dielectrics (ICD)*. 2022, pp. 380–384. DOI: 10.1109/ICD53806.2022.9863543.

[26] H.K.H. Meyer. AC resonant voltage source for PD-measurement. Technical report, SINTEF Energy Research, 2020.

[27] Inc. Tetronix. *Tetronix manual for 5 Series MSO and 6 Series MSO (MSO54, MSO56, MSO58, MSO58LP, MSO64)*. 2018.

[28] F. Vahidi, S. Haegele and S. Tenbohlen. 'A comparison of oil-impregnated pressboard electrical conductivity behavior for two different high density pressboards'. In: *2017 IEEE 19th International Conference on Dielectric Liquids (ICDL)*. 2017, pp. 1–4. DOI: 10.1109/ICDL.2017.8124661.

[29] T. Asokan and S. Bandaru. 'X-wax formation in transformer liquid dielectrics'. In: *IEEE International Conference on Dielectric Liquids, 2005. ICDL 2005.* 2005, pp. 401–404. DOI: 10.1109/ICDL.2005.1490110.

[30] I. G. Folkestad. *Investigation of PD behavior in ceramic substrates under fast repetitive square voltage pulses*. Master's Thesis, Norwegian University of Science and Technology, 2022.

[31] 'From personal communication with scientist Torstein Grav Aakre (at SINTEF Energy Research). Based on non-published works.' In: 2022.

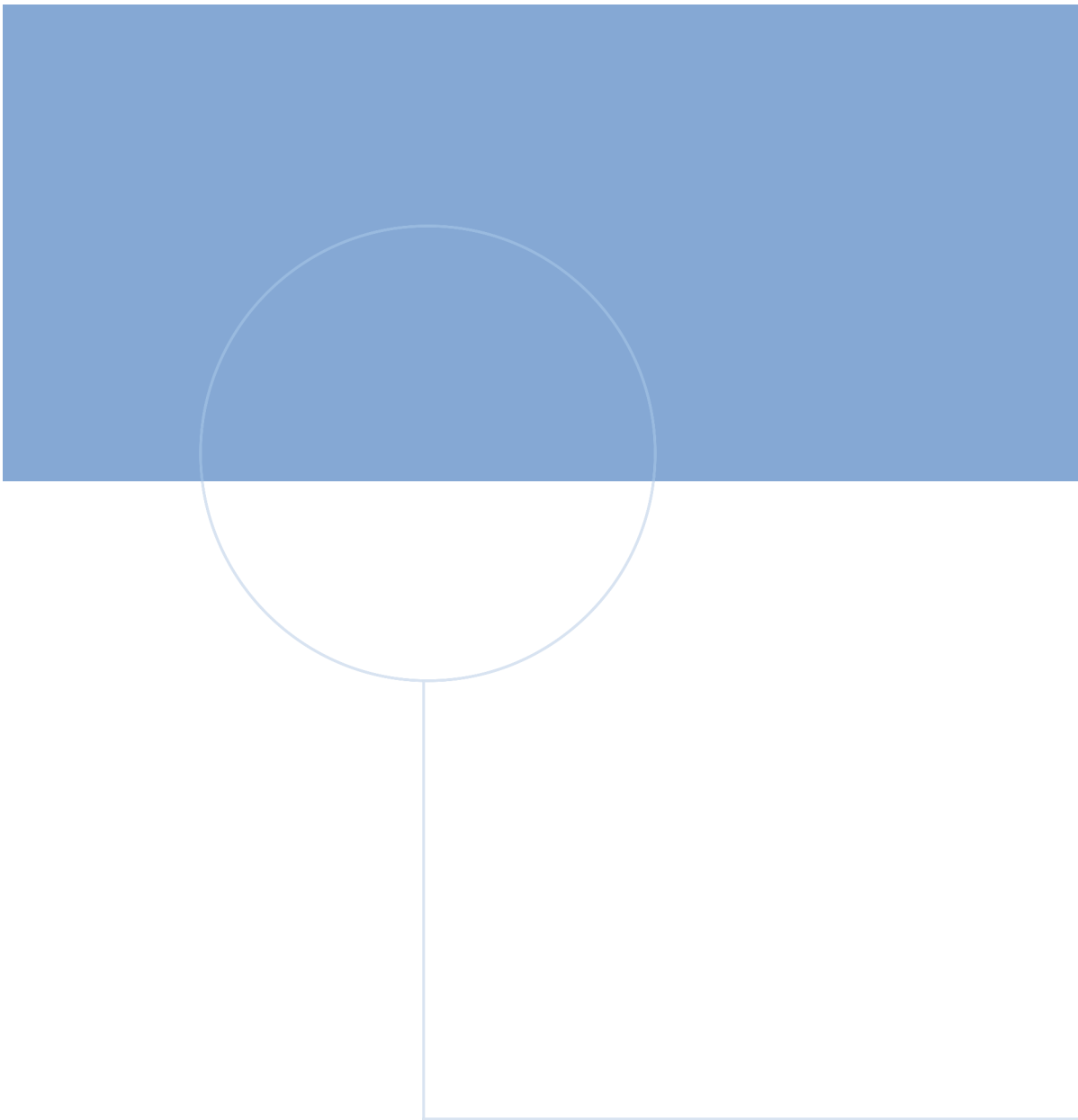

NTNU

Norwegian University of
Science and Technology